4. SITE 733[1]

Shipboard Scientific Party[2]

HOLE 733A

Date occupied: 31 October 1987

Date departed: 2 November 1987

Time on hole: 34 hr

Position: 33°05.30′S, 56°58.68′E

Bottom felt (rig floor, m; drill pipe measurement): 4494.0

Distance between rig floor and sea level (m): 11.10

Water depth (drill pipe measurement from sea level, m): 4482.9

Total depth (rig floor, m): 4510.6

Penetration (m): 16.6

Number of cores (including cores with no recovery): 1

Total length of cored section (m): 16.6

Total core recovered (m): 0.0

Core recovery (%): 0

HOLE 733B

Date occupied: 2 November 1987

Date departed: 3 November 1987

Time on hole: 17 hr

Position: 33°05.30′S, 58°58.68′E

Bottom felt (rig floor, m; drill pipe measurement): 4498.0

Distance between rig floor and sea level (m): 11.10

Water depth (drill pipe measurement from sea level, m): 4486.9

Total depth (rig floor, m): 4502.3

Penetration (m): 4.30

Number of cores (including cores with no recovery): 1

Total length of cored section (m): 4.30

Total core recovered (m): 0.09

Core recovery (%): 2.1

Hard rock:
Depth (mbsf): Not known
Nature: metagabbro and amphibolite rubble

HOLE 733C

Date occupied: 3 November 1987

Date departed: 4 November 1987

Time on hole: 7 hr 15 min

Position: 33°05.30′S, 56°58.68′E

Bottom felt (rig floor, m; drill pipe measurement): 4498.0

Distance between rig floor and sea level (m): 11.10

Water depth (drill pipe measurement from sea level, m): 4486.9

Total depth (rig floor, m): 4503.7

Penetration (m): 5.7

Number of cores (including cores with no recovery): 1

Total length of cored section (m): 5.7

Total core recovered (m): 0.2

Core recovery (%): 3.5

Hard rock:
Depth (mbsf): Not known
Nature: metabasalt and amphibolite rubble

HOLE 733D

Date occupied: 4 November 1987

Date departed: 5 November 1987

Time on hole: 45 hr 15 min

Position: 33°04.92′S, 56°59.39′E

Bottom felt (rig floor, m; drill pipe measurement): 5219.0

Distance between rig floor and sea level (m): 11.10

Water depth (drill pipe measurement from sea level, m): 5207.9

Total depth (rig floor, m): 5242.5

Penetration (m): 23.5

Number of cores (including cores with no recovery): 3

Total length of cored section (m): 8.5

Total core recovered (m): 0.47

Core recovery (%): 5.5

Hard rock:
Depth (mbsf): 20.0
Nature: metagabbro
Measured velocity (km/s): 6.2

Principal results: After failing to drill basement on the median tectonic ridge of the Atlantis II Transform (Site 732), we moved to Site 733, located on the west wall of the transform at about 33°05′S, 56°59′E. Peridotite was dredged from this area during the pre-cruise site survey, and several small benches suitable for guidebase deployment are present. Gravels similar to those encountered at Site 732 were not expected at this site, but we hoped to find peridotite exposed on fault scarps on the transform wall. The main objective of this site was the same as at Site 732: to drill a deep reentry hole in peridotite to determine the lithology and physical properties of mantle material in a major fracture zone.

JOIDES Resolution dropped a beacon at Site 733 at 1351 hr on 31 October 1987. (All times are local unless stated otherwise.) A television/sonar survey of the transform wall located two suitable drilling sites: a flat, sedimented bench in about 4483 m of water and a small, sediment-filled trough about 700 m farther down the slope in about 5208 m of water.

Four holes were drilled in these two locations, the deepest of which penetrated 23.5 meters below seafloor (mbsf). Holes 733A, 733B, and 733C are located on the upper bench and were test holes drilled a few meters apart. A total of 0.29 m of material was obtained for an average recovery of 1%. Hole 733D, drilled in the

[1] Robinson, P. T., Von Herzen, R. P., et al., 1989. *Proc. ODP, Init. Repts.*, 118: College Station, TX (Ocean Drilling Program).

[2] Shipboard Scientific Party is as given in the list of participants preceding the contents.

lower trough, was washed to a depth of 15 m and then drilled to 23.5 mbsf.

The material recovered from Holes 733A, 733B, and 733C consists entirely of fragments of foliated metagabbro and amphibolite, none of which were actually cut by the bit. The size and shape of the fragments indicate that they represent talus deposits, not basement. Foliated metagabbro, amphibolite, and minor basalt were recovered in Hole 733D. Although a whole-round piece of foliated metagabbro was recovered from this hole, it probably came from a boulder in the talus pile, rather than from basement.

The foliated metagabbros and amphibolites were subjected to high-temperature plastic deformation and recrystallized under amphibolite facies conditions. Two types of metagabbro are present: a green variety composed chiefly of amphibole and plagioclase and a brown variety that contains predominantly pyroxene and plagioclase. We believe that the protoliths for both varieties were orthopyroxene-rich ferrogabbro. The amphibolite is strongly foliated and consists of amphibole, plagioclase, and epidote. In the metabasalt, actinolite replaces most of the mafic minerals and some of the groundmass plagioclase. Chlorite and epidote are absent, which suggests upper-greenschist to lower-amphibolite facies conditions of metamorphism.

The metagabbros have remanent magnetic intensities similar to those of fresh and altered gabbro from the Mid-Atlantic Ridge, but their initial susceptibilities are much lower. The stable magnetic inclinations from both oriented samples are −20°; however, this has little significance because the core was probably recovered from a boulder in the talus overlying basement at this site.

Measured grain densities of the metagabbros are 2.87 and 2.96 g/cm^3, within the range of expected values. However, the compressional-wave velocities (6.14–6.24 km/s) are somewhat higher than those for metagabbros from other fracture zones. Variability may be due to differing types or amounts of alteration or to varying proportions of microcracks.

Thermal conductivities range from 1.98 to 2.16 W/m/K and vary systematically when measured parallel or normal to the foliation. The mean conductivity of 2.10 W/m/K is typical for diabase and gabbro. We believe that the small observed anisotropy reflects the preferred mineral orientations.

Because basement was not reached in these holes and drilling conditions were not promising, another site was selected for a test spud-in. *JOIDES Resolution* departed Site 733 at 2130 hr on 5 November.

BACKGROUND AND SCIENTIFIC OBJECTIVES

A primary goal of Leg 118 was to sample an *in-situ* section of upper mantle peridotite in the Atlantis II Fracture Zone. The first attempt to spud into basement on the median ridge of the transform at Site 732 failed because the ridge crest is mantled by an unknown thickness of rubble or breccia. Consequently, Site 733 was selected for a television/sonar survey and test spud-in to locate a drillable outcrop of serpentinized peridotite. Site 733 is located on the west transform wall at 33°05′S, 56°59′E (Fig. 1), in an area where several dredge hauls recovered peridotite during the pre-cruise site survey. We hoped that peridotite might crop out along fault scarps on the transform wall and that small benches might be present on which the guidebase could be deployed. We also expected that the rubble or breccia covering the floor of the transform and the crest of the median ridge might be less abundant on the transform walls. The main objectives of this site were the same as those at Site 732: to drill a deep reentry hole in peridotite for determining lithology and physical properties of mantle material in a major fracture zone.

GEOLOGIC AND TECTONIC SETTING

Site 733 is located on the west wall of the Atlantis II Fracture Zone at 33°05′S, 56°59′E (Fig. 1). In this area, the transform wall has a relief of about 2200 m, measured from the break in slope at the top to the valley floor. Several flat, elongated benches appear to mark the intersection of a cross structure with the transform wall. North of this structure, the slope of the wall is considerably lower than average, and the upper slope break is farther west. From several dredge hauls just north of Site 733, abundant peridotite and lesser amounts of basalt and diabase were recovered. The area was selected for closer investigation and drilling because of (1) its proximity to those dredge hauls, (2) the presence of flat benches suitable for guidebase deployment, and (3) the absence of landslide morphology.

Two television/sonar survey lines were run downslope across several benches identified from the pre-cruise site survey Sea Beam map. The surveys revealed slopes largely covered with rubble and minor sediment and relatively flat benches covered with uniform, fine-grained sediment. Two locations were selected for test spud-ins: one on a bench at about 4500 m water depth, the other in a sedimented trough at about 5200 m. Both of these sites were topographically suitable for guidebase deployment. We were unable to locate good bare-rock sites; however, we believed that basement might occur at shallow levels beneath the sedimented areas.

OPERATIONS

Introduction

Site-survey data for this general region, acquired in October 1986 (*Conrad* 27-09 cruise, H. Dick, pers. comm., 1987), formed the primary basis for selecting this site. We did not expect to encounter the type of sedimentary rubble on the west wall of the transform that plagued drilling at Site 732. Sea Beam bathymetry data from the site survey showed several small topographic benches, 0.5 to 1 km wide, perched on the otherwise steep slope of the west wall of the transform in this region. We believed that the existence of such benches would assure sufficiently flat locations for deployment of the hard-rock guidebase, if conditions were otherwise appropriate. The beacon location was planned to include several such benches at depths of about 4200, 4500, and 5200 m, which were within range for a detailed survey. The site survey included two dredge hauls (DR-34 and DR-35), located on the wall 3 to 4 nmi to the north, from which mostly peridotite was recovered. Thus, we believed that this area offered good opportunities for drilling and for establishing a deep hole in ultrabasic rock.

Approach to Site 733

As on the approach to Site 732, the seismic system that was streamed behind the ship was the primary source of bathymetric data for comparison with the Sea Beam maps, as the higher-frequency depth sounders of the ship are practically inoperative at normal ship speeds. We approached the site from the north at 5 to 6 kt, under global positioning system (GPS) navigation control, and a small track pattern (Fig. 2) was surveyed to establish continuity with the Sea Beam contour map. The topographic benches of possible interest for drilling were crossed, and we determined before dropping the beacon that the generally north-south trending contours of the Sea Beam map were displaced to the east by about 0.3 to 0.4 min of longitude, with respect to GPS navigation. Continuity in the north-south direction was more difficult to determine, but it was probably less that 0.5 min of latitude.

At the completion of the brief 1.5-hr survey, the beacon (SN-413) was dropped at 1400 hr (5.5 hr after leaving Site 732), 31 October 1987, at 33°05.30′S, 56°58.87′E. We determined that the beacon depth was 4075 m by observing it with the television/sonar. This depth was somewhat less than that estimated from the ship's seismic profiling system (Fig. 3).

Television/Sonar Survey

Television/sonar surveys to determine the geological nature of the bottom and its lateral variability occupied about 10 hr.

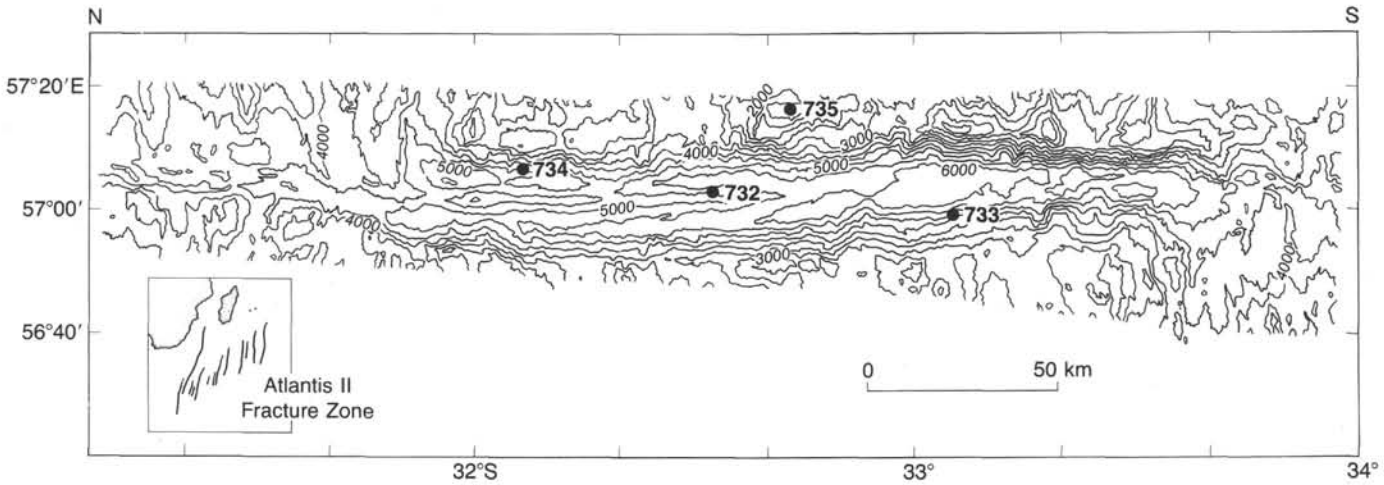

Figure 1. Bathymetry map at 500-m contour intervals of the Atlantis II Fracture Zone, Southwest Indian Ridge, showing Leg 118 drill sites. Survey from *Conrad* cruise 27-09, 1986 (H. Dick, Chief Scientist, with D. Gallo and R. Tyce).

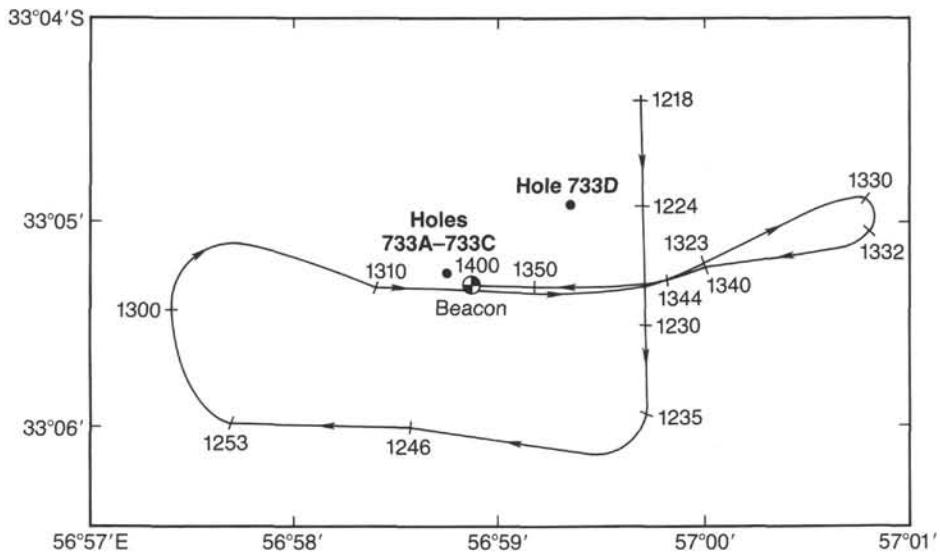

Figure 2. Ship track line followed before deployment of beacon at Site 733 on 31 October 1987. Times along track are local (UTC + 4 hr). Drill-hole locations are also shown.

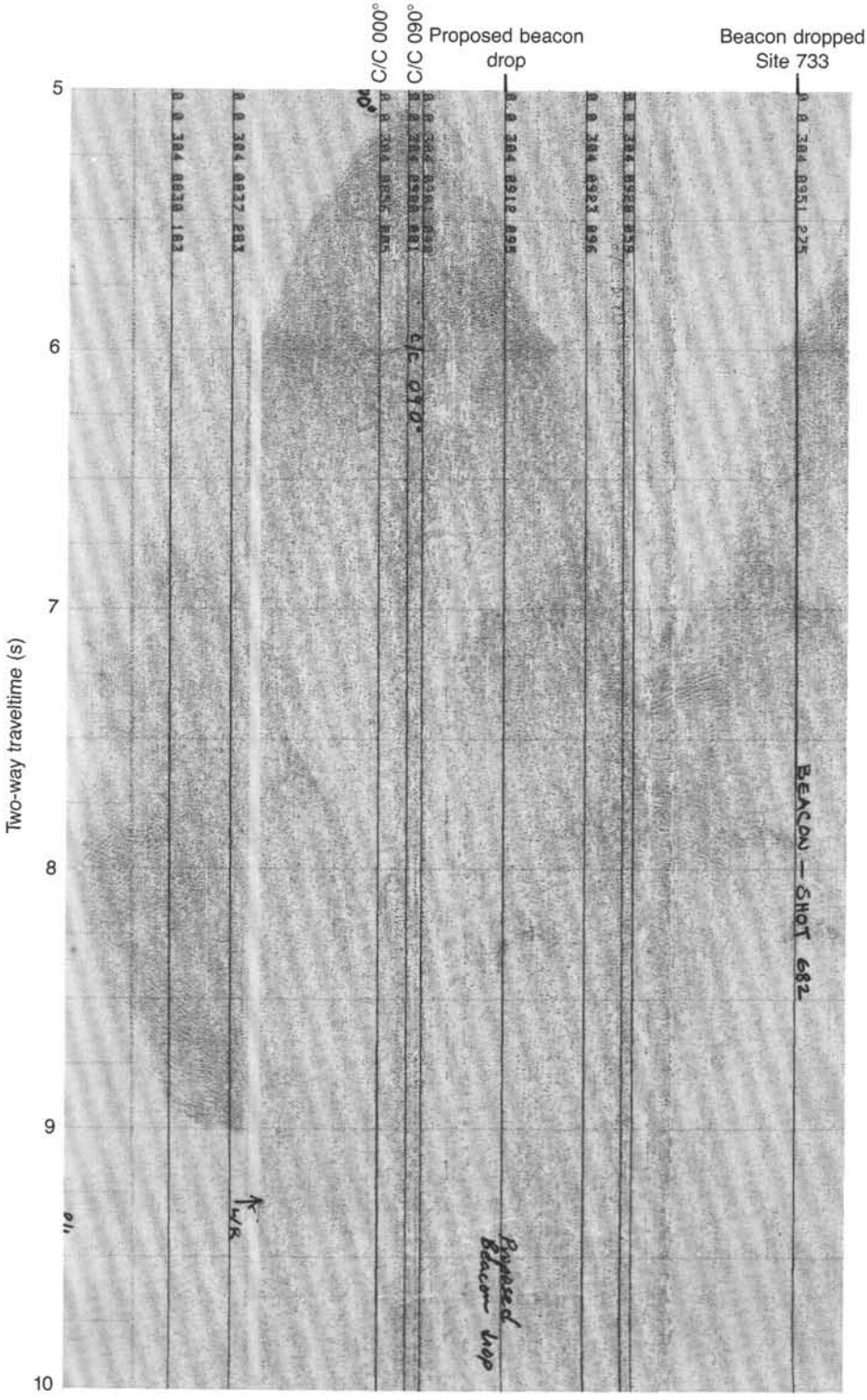

Figure 3. Seismic-reflection profile recorded during the approach to Site 733 between about 0825 and 1000 hr (UTC), 31 October 1987. Note that the initial part of the recording (until 0838 hr) is reversed as a result of a wrong recorder switch setting. Time interval of recording after each "shot" is between 5 and 10 s, and ship's speed was about 5 to 6 kt.

Methodology and techniques used were the same as those described in the Site 732 "Operations" section (this volume). At Site 733, the survey tracks were configured differently for several reasons. First, topographic contours are not oriented exactly north-south, but rather are aligned somewhat east of south and are associated with an increase in width toward the north between walls of the transform in this region. To maintain the television/sonar near the bottom, while avoiding contact with any irregularities along the track, we found it desirable to run the profile lines downslope. Also, the weather was relatively rough at the time of the survey, and the configuration of the ship's winch at the moon pool required us to align the ship with

the stern heading in the direction in which the survey lines were run. Fortunately, all these constraints were operationally compatible with each other during the survey, so that we were able to perform the survey efficiently.

Two nearly parallel survey lines, about 4 km in length and separated by 400 to 500 m, were run in a southwest-northeast direction on opposite sides of the beacon (Fig. 4). These profile lines crossed the benches we expected to find from Sea Beam maps and otherwise showed relatively steep slopes (25° to 35°). Sediments, rubble, and large boulders in various locations were seen on the benches. Some of the benches, especially the one identified at about 5200 m, showed uplifted topography (as much as 100 m) and large rounded boulders (dimensions up to 15 m) on their outer lips, then dropping off to steep slopes below. The steep slopes between or below the benches commonly have exposures of massive rock or rubble. Some of the massive rock and large boulders have relatively planar surfaces and angular intersections, although smooth surfaces and rounded large boulders also are common.

Several holes were drilled at each of two sites: one on the bench at a depth of about 4500 m and the other at 5200 m (Table 1). At each hole drilling was stopped by rubble or by a slow rate of penetration, and core recovery was minimal.

Hole 733A

The positive displacement coring motor with a C-4 bit was picked up, and pipe was lowered to the seafloor. The television/sonar failed; it took 11 hr to repair it. Later, while the television/sonar was being lowered again, the on-bottom beacon failed, forcing us to launch the standby beacon (SN-353). However, approximately 20 min after its launch, the beacon's frequency changed and the signal became unreliable. The original beacon (SN-413) then began to recover, but 14 hr later it failed again, and a third beacon (SN-411) was deployed. This one landed 800 m north of the ship, but because of its distance provided only marginal positioning capability. Fortunately, the original beacon (SN-413) then began to function again.

Eventually, dynamic-positioning personnel concluded that the two operating beacons were being knocked down by a bottom current and that their full signal was not reaching the ship. The second beacon (SN-353) apparently suffered an unknown electronic failure.

The bottom was sighted by the television/sonar at 4494 meters below rigfloor (mbrf). A core was cut to 16.6 meters below seafloor (mbsf) in 3 hr (Table 1). The hole was stable except for an overpull of 60,000 lb at 10 mbsf. Four runs with the wireline were required to latch the core barrel; a piece of rubber from the drill-pipe stabbing guide had jammed in the latch finger, preventing us from engaging the overshot. Fortunately, the same piece of rubber had jammed the core-barrel fishing neck in the overshot, which resulted in our recovering the barrel. While fishing for the core barrel, cuttings apparently entered the mud motor, making circulation impossible. The bit was raised above the mud line, which fortunately caused the blockage to fall out. No core was recovered.

Hole 733B

The bit tagged bottom at 4498 mbrf. The hole was stable but drilling was very difficult. The hole was cored to 4.3 mbsf in 11.25 hr (Table 1). A total of 0.09 m of metagabbro and amphibolite was recovered.

Hole 733C

One 5.7-m-long core was cut in 11.75 hr (Table 1). A total of 0.2 m of metabasalt and amphibolite was recovered. We decided to move to another site in an attempt to find rock that could be drilled more easily.

Hole 733D

The next location was another sediment-filled basin, about 700 m down the transform wall from Holes 733A through 733C. We observed from the television/sonar that the bit touched a soft seafloor at 5219 mbrf. The bit took little or no weight for the first 15 mbsf that was washed (Table 1). The next 5 m were drilled at a reasonable rate of penetration. Extremely hard material was then encountered. From the first core at 15–22 mbsf, we recovered 0.41 m of gabbro, but the second core (at 22–23.5 mbsf) contained almost nothing. After 23 hr of rotation, the hole was abandoned, 8.5 m into the hard material. After 44 hr of rotation, the bit reached the surface completely destroyed.

Should ODP return to the west wall site, the area around Hole 733D should be considered an operating area. The 15 m of sediment offers the opportunity for a casing wash or drill-in. Sediments do not appear to contain rocks that might fall into the hole, and the formation below is stable but very hard.

Most of the drilling at Site 733 was slow. This may reflect in part the apparently widespread occurrence of the strongly foliated and recrystallized metagabbro and amphibolite, but more likely is a consequence of the low weight (5000 to 10,000 lb) that could be applied to the bit in these shallow, nearly bare-rock, holes.

Because of the lack of success in finding massive outcrops of easily drilled peridotite on the west wall, the shipboard scientific party elected to move to a site on the east wall (Site 734), where peridotite had been dredged. *JOIDES Resolution* departed Site 733 at 2130 hr on 5 November 1987 and traveled about 60 nmi north and a little east to Site 734.

LITHOSTRATIGRAPHY

Metagabbro, amphibolite, and basalt were recovered in three of the four holes drilled at Site 733. Drilling in Hole 733D washed through 15 m of soft sediments, and the television camera showed at least a few centimeters of sediment at each of the other holes. One foliated amphibolite was recovered in Core 118-733B-1D, and a similar amphibolite and an altered basalt were recovered in Core 118-733C-1D. The foliation in the first amphibolite is defined by alternating layers of green amphibole and plagioclase; the protolith is assumed to have been an amphibolitized gabbro, but the only remaining minerals of igneous origin are plagioclase porphyroclasts. The second amphibolite recovered was oriented vertically in the core barrel and has a foliation dipping about 80°. It also had an amphibolitized gabbroic protolith. The first clearly cored igneous or metamorphic samples were recovered in Core 118-733D-1D, in which a 20-cm-long section of medium-grained, two-pyroxene metagabbro was recovered above about 20 cm of a coarse, two-pyroxene metagabbro or metamorphosed gabbronorite (Fig. 5).

The gabbroic samples are intensely deformed and highly recrystallized, with common deformation twins and stretched and fractured grains. Foliation in the coarse gabbro dips 45°, as does the stretching lineation within the foliation. The transition from medium- to coarse-grained gabbro at 20–22 cm in Core 118-733D-1D may derive from an original layering, but may also reflect greater strain in the finer-grained part.

Two angular pebbles were recovered in Core 118-733D-2D: one a fine-grained metabasalt having an amphibolitized matrix and one a foliated amphibolite. These pebbles were not cored and we do not know their position relative to the metagabbro. A few fragments of amphibolitized metagabbro, one cut by a

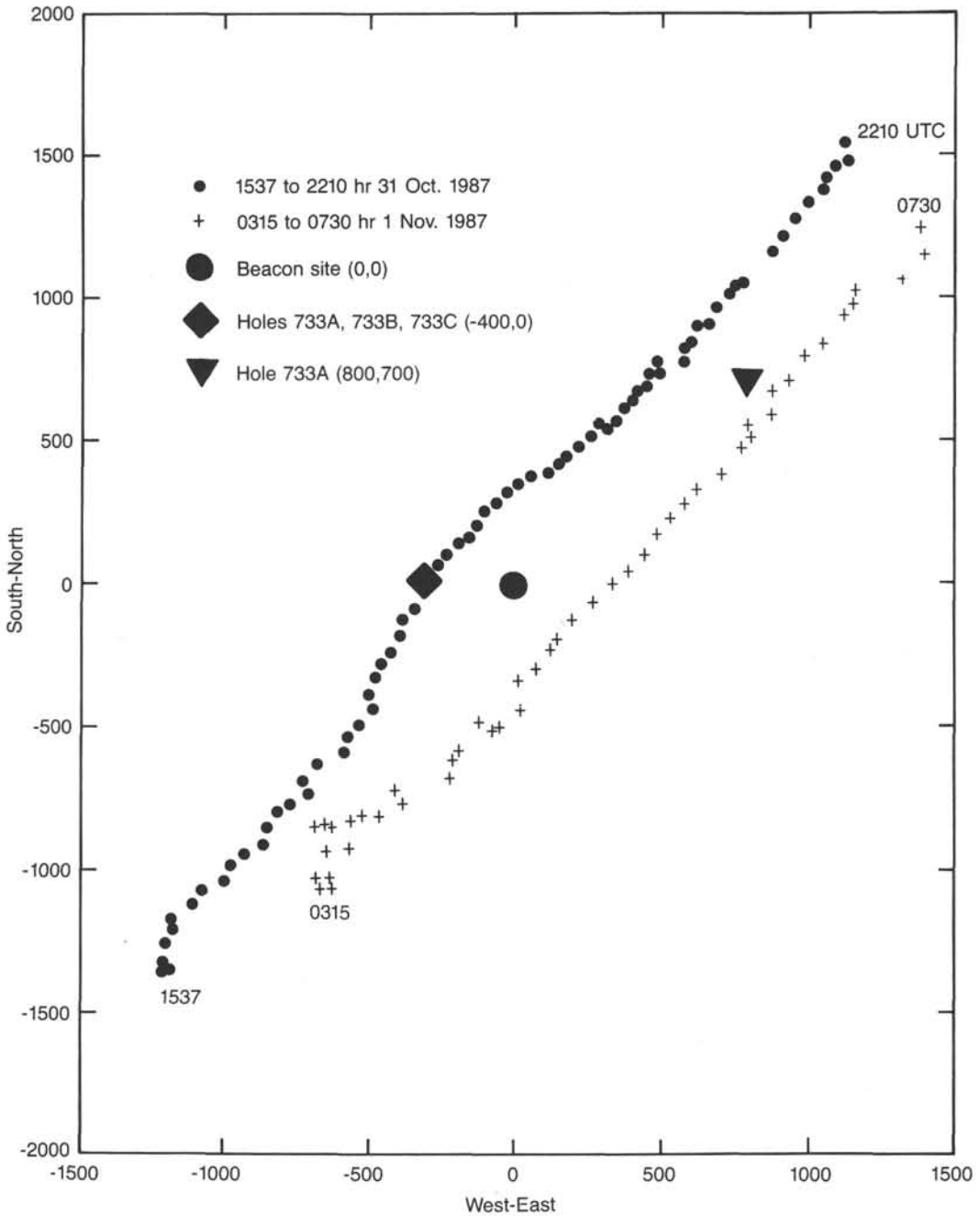

Figure 4. Plot of navigation for television/sonar survey at Site 733. Symbols are positions at nominal 5-min intervals over various time periods (UTC) during survey, as indicated. The beacon site is located at 33°05.30′S, 56°58.87′E, and drill-hole locations are as shown. Axis dimensions in meters from beacon.

Table 1. Site 733 coring summary.

Core	Date (Nov. 1987)	Time (local)	Total depth[a] (m)	Depth (mbsf)	Length advanced (m)	Length cored (m)	Length recovered (m)	Recovery (%)
118-733A-1D	2	2300	4494.0–4510.6	0–16.6	16.6	16.6	0	0
733B-1D	3	1555	4498.0–4502.3	0–4.3	4.3	4.3	0.09	2.1
733C-1D	4	0115	4498.0–4503.7	0–5.7	5.7	5.7	0.20	3.5
733D, Wash			5219.0–5234.0	0–15.0	15.0	0	0	—
733D-1D	5	0115	5234.0–5241.0	15.0–22.0	7.0	7.0	0.41	2.7
733D-2D	5	2200	5241.0–5242.5	22.0–23.5	1.5	1.5	0.05	3.3
[b]733D-3B	5	2200	5242.5–5242.5	23.5–23.5	0	0	0.01	—

[a] Determined from drill pipe length below rig floor.
[b] As fragments recovered from bit; not cored.

Figure 5. Foliated metagabbro from Core 118-733D-1D (Piece 3B).

small basaltic dikelet, were recovered from the bit at Hole 733D (Core 118-733D-3B).

PRIMARY MINERALOGY

Introduction

Samples from Site 733 include cored, foliated metagabbro (Sample 118-733D-1D-1, 0–46 cm, Pieces 1, 2A, 2B, 3A, and 3B) and a number of randomly collected fragments of metabasalt (Sample 118-733C-1D-1, 0–7 cm, Piece 1), foliated metagabbro and amphibolite with a gabbro protolith (Samples 118-733B-1D-1, 0–9 cm, Piece 1; 118-733C-1D-1, 10–20 cm, Piece 2; 118-733D-2D-1, 0–4 cm, Piece 1; and 118-733D-3B-1, 0–5 cm, Piece 1), and amphibolite with protolith unclear (Sample 118-733D-2D-1, 5–8 cm, Piece 2).

All these samples were metamorphosed at temperatures sufficient to produce hornblende and/or actinolite. Very minor amounts of later low-temperature alteration produced traces of clay minerals. In addition, all samples except the basalt fragment (Sample 118-733C-1D-1, 0–7 cm, Piece 1) are foliated.

The primary igneous mineralogy of the metagabbros, obscured by high-temperature metamorphism, suggests an orthopyroxene-bearing gabbro. The metagabbros can be grouped into predominantly amphibole- and plagioclase-bearing rocks (amphibolites or green metagabbros), and predominantly pyroxene and plagioclase-bearing rocks (brown metagabbros). In the green metagabbros, fractured plagioclase porphyroclasts are the only relicts of primary igneous minerals. The primary mafic minerals have been entirely replaced by amphiboles. In the brown metagabbros, the igneous plagioclase and pyroxene were partially recrystallized during plastic deformation: the temperature conditions during this deformation thus were constrained by the stability of the orthopyroxene plus clinopyroxene plus plagioclase neoblasts.

Here, we describe the primary igneous mineral assemblages of the Site 733 samples and how they were obscured by high-temperature metamorphism under dynamic conditions. In the "Metamorphism and Deformation" section (this chapter), we describe the metamorphic mineral assemblages and the development of the deformation fabric. The metamorphic assemblages can be characterized roughly as pre-deformation, syndeformation, and post-deformation on the basis of petrographic observations and textures.

Petrography

The samples recovered in Holes 733B, 733C, and 733D are variously deformed and metamorphosed gabbros and a basalt. To establish their protoliths, we found it necessary to interpret the pattern of mineral replacement so that the primary abundances could be estimated from secondary mineral assemblages. The recovered samples can be divided into two categories: (1) samples having relict primary phases coexisting with late low- to medium-grade metamorphic assemblages (termed brown gabbros or foliated metagabbros, see "Metamorphism and Deformation" section, Hole 733D, this chapter), and (2) samples having mainly a metamorphic mineralogy (termed amphibolites, see "Metamorphism and Deformation" section, Holes 733B, 733C, and 733D, this chapter). The textures and inferred relationships among relict primary minerals and their metamorphic replacements are presented as follows:

1. *Plagioclase*. This is the most abundant phase in nearly all samples. Replacement minerals are typically plagioclase neoblasts that result from recrystallization under high-temperature deformation (Samples 118-733D-1D-1, 38–45 cm, Piece 3B, and 118-733D-2D-1, 4–7 cm, Piece 2). Small amounts of epidote (Sample 118-733-2D-1, 4–7 cm, Piece 2) and chlorite (Sample 118-733B-1D-1, 38–45 cm, Piece 3B) also replace plagioclase.

2. *Clinopyroxene*. This is the second most abundant phase in the samples. In the gabbroic samples, clinopyroxene porphyroclasts (augite) are partially recrystallized into small neoblasts (probably more diopsidic in composition; Samples 118-733D-1D-1, 35–37 cm, Piece 3B, and 118-733D-1D-1, 14–15 cm, Piece 2A). Amphibole (either hornblende or actinolite, Samples 118-733D-1D-1, 15–23 cm, Piece 2B, and 118-733D-2D-1, 0–4 cm, Piece 1) and lesser quantities of chlorite (Sample 118-733D-1D-1, 35–37 cm, Piece 3B) also replace clinopyroxene or the green hornblende pseudomorphs of clinopyroxene. Clinopyroxene porphyroclasts contain numerous tiny brown amphibole in-

clusions (Samples 118-733D-1D-1, 14–15 cm, Piece 2A; 118-733D-1D-1, 15–23 cm, Piece 2B; and 118-733D-1D-1, 35–37 cm, Piece 3B).

3. *Orthopyroxene*. This is the third most abundant primary phase in the samples examined. Orthopyroxene porphyroclasts (hypersthene) are only slightly recrystallized to fine-grained neoblasts (Sample 118-733D-1D-1, 15–23 cm, Piece 2B). Cummingtonite or tremolite (with some talc?) is the main replacing phase (Sample 118-733D-1D-1, 38–45 cm, Piece 3B). Lesser amounts of magnesian chlorite and rare actinolite also are present (Sample 118-733D-1D-1, 35–37 cm, Piece 3B).

4. *Opaque phases*. Ilmenite and/or titaniferous magnetite are the most abundant primary opaque minerals. They are partly replaced by magnetite, chlorite, sphene, rutile (Samples 118-733D-1D-1, 14–15 cm, Piece 2A, and 118-733D-1D-1, 15–23 cm, Piece 2B), and hematite (Sample 118-733D-1D-1, 38–45 cm, Piece 3B).

5. *Brown amphibole*. This mineral is, by analogy to other oceanic gabbros, probably kaersutitic pargasite or titaniferous hornblende. It is partly recrystallized to pale brown amphibole (Sample 118-733D-1D-1, 1–4 cm, Piece 1), actinolite (Sample 118-733C-1D-1, 10–12 cm, Piece 2), and green hornblende (Sample 118-733D-1D-1, 2–5 cm, Piece 1). We believe that the limpid, dark brown, well-developed amphiboles are of magmatic origin and probably have crystallized from hydrous intercumulus liquids (along with ilmenite). They occur as small blebs in clinopyroxene porphyroclasts or as thin linings at the outermost margins of the prophyroclasts and ilmenite. Some of these amphiboles may have formed contemporaneously with high-temperature metamorphism. This metamorphism allowed small amounts of high-temperature brown amphibole (stable under these conditions) to recrystallize into neoblast mosaics or around the margins of the clinopyroxenes.

Using the information above, the original mineral percentages of the highly altered, as well as the less altered, samples can be estimated (Table 2). The protoliths fall into four groups: (1) gabbronorite, (2) orthopyroxene-poor gabbro, (3) fine-grained microgabbro or diabase, (4) metabasalt. The first two groups are clearly separated in a ternary plot of the modal proportions of original plagioclase, clinopyroxene, and orthopyroxene (Fig. 6 and Table 2).

Gabbronorite protoliths (Group 1) include Samples 118-733D-1D-1, 12–14 cm, Piece 2A; 118-733D-1D-1, 15–23 cm, Piece 2B; 118-733D-1D-1, 38–45 cm, Piece 3B; and 118-733D-2D-1, 0–4 cm, Piece 1. These are mafic to leucocratic (color index [c.i.]: 40–48 and 29–30, respectively), depending on the modal proportion of plagioclase (Figs. 7 and 8). The pyroxene ratio (clinopyroxene:orthopyroxene) varies from 1:1 to more than 3:2. Sample 118-733D-1D-1, 15–23 cm, Piece 2B, contains a conspicuous contact between foliated leucogabbronorite (c.i. = 29) and foliated gabbronorite (c.i. = 48; Fig. 7). The average grain size of the leucogabbronorite is 6 mm and that of the gabbronorite is 2 mm. The leucogabbronorite contains less ilmenite and brown amphibole (0.4 and 0.7 vol%, respectively) than the gabbronorite (2 and 3.5 vol%, respectively; see Table 2). A symplectiticlike intergrowth in orthopyroxene suggests that a small amount of olivine (<1%) may also have been present in the gabbronorite. These data suggest that the contact is a boundary between two cumulate layers. This layering was probably highly transposed by a strong foliation that resulted from high-temperature plastic deformation (see "Metamorphism and Deformation" section, this chapter, and Fig. 8). Phase layering, marked by variations in the abundance of plagioclase, is typical of layered complexes. The occurrence of cumulus orthopyroxene and the low abundance of brown amphiboles and ilmenite suggest that the Site 733 gabbros were derived from a moderately fractionated tholeiitic liquid (low titanium and iron enrichment).

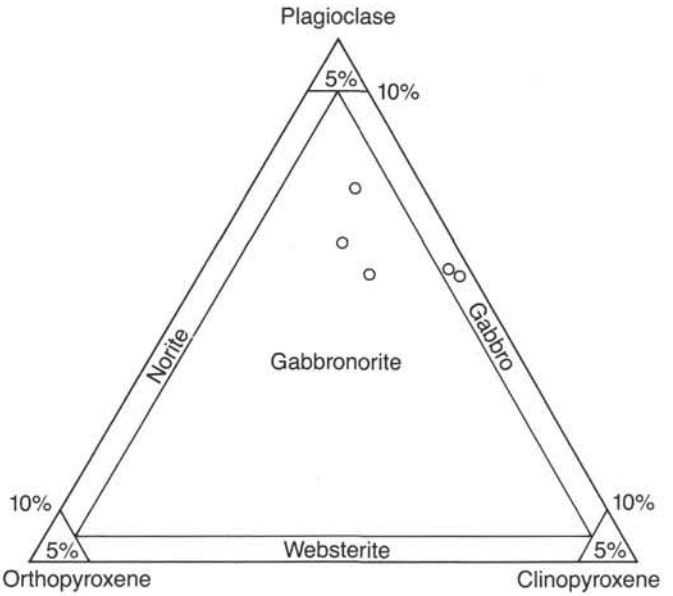

Figure 6. Triangular plot showing the classification of gabbroic rocks. Open circles indicate modal compositions of gabbronorites and gabbros in Table 2. Diagram after Streckeisen (1976).

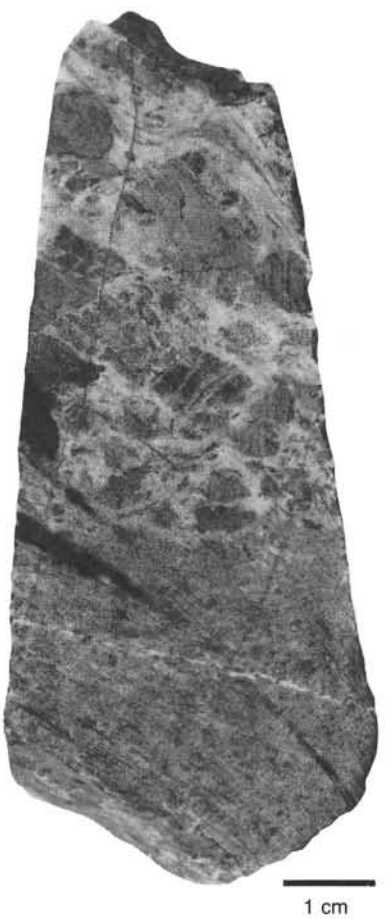

Figure 7. Photograph of Sample 118-733D-1D-1, 15–23 cm, Piece 2B, showing the contact between leucogabbronorite (lower half of the sample) and gabbronorite (upper half of the sample). The point-counted area is located across this contact (see Table 2).

Table 2. Modal compositions of samples from Section 11B-733D-1D-1.

Intervals (cm):	2–5	12–14	15–23 Observed mineralogy A	15–23 Observed mineralogy B	35–37
Relict Primary Mineralogy					
Plagioclase	12.2	17.4	38.3	6.9	14.8
Clinopyroxene	14.9	14.8	7.7	4.1	28.4
Orthopyroxene	0.5	15.2	10.3	10.5	1.4
Opaque phases	—	0.4	0.2	1.0	0.1
Brown amphibole	2.9	0.2	0.7	3.3	0.9
Secondary Mineralogy					
Neoblasts					
Plagioclase	42.3	43.0	32.3	45.2	39.5
Clinopyroxene	6.9	3.5	0.3	7.5	12.8
Orthopyroxene	—	0.0	0.8	5.4	0.0
Replacement phases					
[1]Amphiboles	18.4	4.5	8.2	14.9	1.8
Magnetite	1.2	0.8	—	—	0.3
Clay, chlorite, other phases	1.1	0.2	1.0	0.8	0.0
Original Primary Mineralogy					
Plagioclase	54.5	60.6	70.6	52.1	54.3
Clinopyroxene	39.4	20.4	17.2	26.5	42.7
Orthopyroxene	3.2	18.2	11.1	15.9	2.0
Ilmenite	—	0.4	0.4	2.0	0.1
Brown amphibole	2.9	0.2	0.7	3.5	0.9
Color index	45.5	39.4	29.4	47.9	45.7

[1] Includes mostly actinolite and lesser amounts of cummingtonite and green hornblende.

Note: Points counted by thin section: 2000 at 0.4 mm spacing; corresponding piece number to interval of thin section: 2–5 = Pc. 1; 12–14 = Pc. 2A; 15–23 = Pc. 2B; 35–37 = Pc. 3B; color index is the sum of modal mafic and opaque phases.

Figure 8. Photograph of the entire thin section from Sample 118-733D-1D-1, 15 -23 cm, Piece 2B. P = plagioclase porphyroclasts, Pn = plagioclase neoblasts; C = clinopyroxene porphyroclasts, Cn = clinopyroxene neoblasts; O = orthopyroxene porphyroclasts. The arrow points toward the top of the core. The bar scale is 1 cm long. Note the contact and the strong deformation in the upper part of the sample.

The gabbro protolith (Group 2) includes four samples: 118-733B-1D-1, 1–4 cm, Piece 1; 118-733C-1D-1, 10–12 cm, Piece 2; 118-733D-1D-1, 2–5 cm, Piece 1; and 118-733D-1D-1, 35–37 cm, Piece 3B. The gabbros are exclusively mafic rocks (c.i. = 46–55) composed of plagioclase, clinopyroxene, and accessory orthopyroxene (Fig. 9). The modal contents of brown amphibole and ilmenite are lower than for the gabbronorites (<2.9 and <0.1 vol%, respectively). In these gabbros, the pyroxene ratio is high (13:1 to 22:1) and relatively constant. The mineralogical data suggest that the gabbros represent mafic layers in a cumulate sequence composed largely of gabbronorite. Primary mineral assemblages suggest a formation depth of 3 to 5 km (Cann, 1979).

A single sample (Sample 118-733D-2D-1, 4–7 cm, Piece 2) of fine-grained mafic rock makes up Group 3. This sample is highly recrystallized and metamorphosed with no relict primary phases. We believe that the percentage of brownish-green hornblende reflects the pyroxene content of the protolith. The grain size of the rock (0.015–0.13 mm) and its metamorphic minerals suggest that the protolith was a fine- to medium-grained microgabbro or a diabase that crystallized at a shallower level than the metagabbros of Groups 1 and 2.

The one sample in Group 4 (Sample 118-733B-1D-1, 0–3 cm, Piece 1) is a porphyritic metabasalt containing abundant green-brown, actinolitic hornblende. However, its primary texture is very well preserved. Plagioclase (10 vol%) and olivine pseudomorphs (initially 2 vol%) are set in a previous clinopyroxene-rich groundmass. This sample obviously originated at a higher level than the gabbronorites, gabbros, and probably the microgabbro (or diabase).

METAMORPHISM AND DEFORMATION

In the green metagabbros (Samples 118-733B-1D-1, 1–4 cm., Piece 1; 118-733C-1D-1, 10–12 cm., Piece 2; and 118-733D-3B-1, 0–5 cm, Piece 1), the igneous pyroxenes of the protolith are entirely replaced by large crystals of pale green to brownish-green amphibole. Some pale green to brownish-green hornblende pseudomorphs preserve the cleavage of the original igneous clinopyroxene (Fig. 10). Within these hornblende pseudomorphs, small blebs of reddish-brown hornblende are optically identical to the hornblende observed in the fresh clinopyroxene of the brown metagabbros. These were interpreted as probably igneous (see "Primary Mineralogy" section, this chapter). Large grains of fibrous cummingtonite (identified optically) probably replace the original igneous orthopyroxene (Fig. 10). The only relicts of the primary igneous mineral assemblage are partly recrystallized and fractured plagioclase porphyroclasts (Fig. 11).

The foliation is defined by stretched crystals of hornblende (Fig. 12) and cummingtonite (Fig. 10). Most of this stretching is

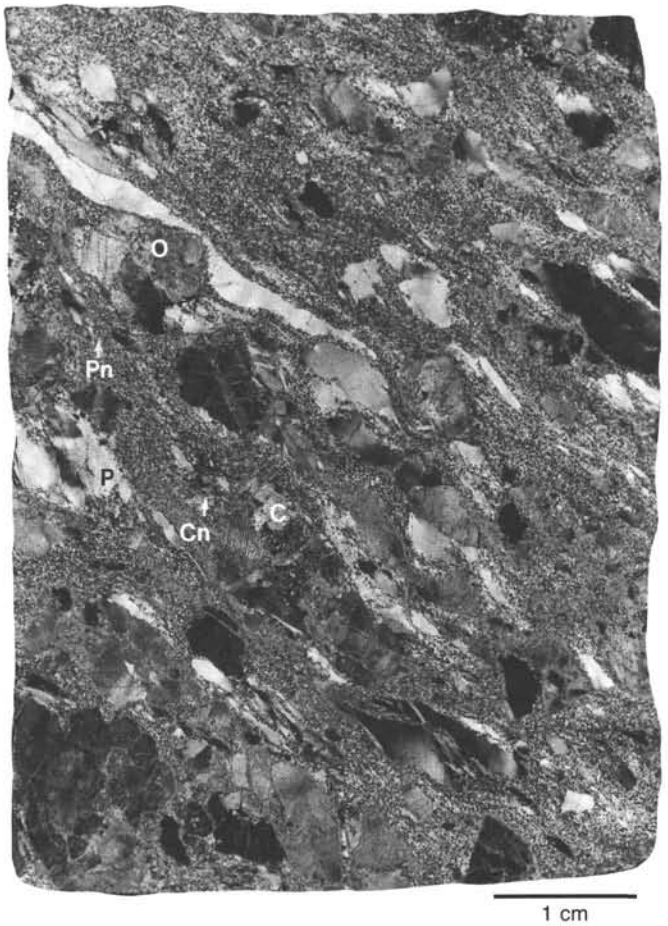

Figure 9. Photograph of the entire thin section from Sample 118-733D-1D-1, 2–5 cm, Piece 1. Explanation as in Figure 8. The bar scale is 1 cm long. Note the strong deformation and elongation of the crystals.

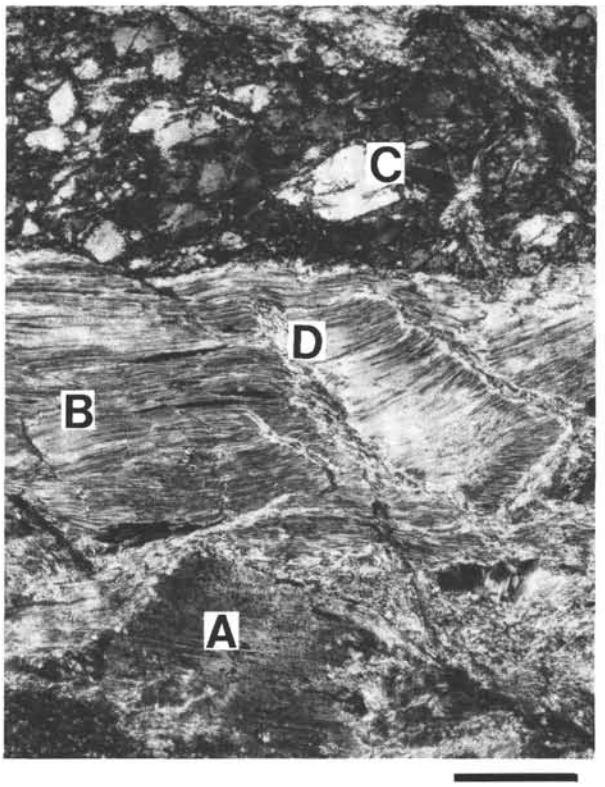

Figure 10. Green metagabbro, Sample 118-733C-1D-1, 10–20 cm, Piece 2. Hornblende pseudomorph of igneous clinopyroxene (A) and cummingtonite replacing igneous orthopyroxene (B). Note the crushed plagioclase (C) and the extensional fractures in the cummingtonite (D). These fractures, filled with a fine-grained amphibole, make a 45° to 60° angle with the foliation (horizontal in the photograph) and indicate that extension occurred in a dextral-shearing regime. Crossed nicols, plane light. Scale bar is 0.5 mm.

accommodated by fractures filled with small grains of a secondary amphibole that is optically identical to the fractured porphyroclasts (Fig. 10). However, fracturing alone cannot account for the preferred orientation of most amphiboles having their long axis in or near the foliation plane (Figs. 10 and 12). Plastic deformation and synkinematic growth of the amphibole porphyroclasts thus may have occurred at an early stage of the deformation. Alternatively, this preferred orientation could have been inherited through pseudomorphic replacement of plastically deformed and stretched pyroxenes. We prefer the first hypothesis because the relict plagioclase porphyroclasts in both samples lack well-developed mechanical twins and do not seem to have been deformed at the very high temperatures required to plastically deform pyroxenes.

The fracturing and partial replacement of amphibole porphyroclasts by smaller grains of an optically identical amphibole was accompanied by crushing (Figs. 10 and 11) and recrystallization (Fig. 12) of the plagioclase porphyroclasts.

In Sample 118-733B-1D-1, 1–4 cm, Piece 1, the next identifiable discrete event is static alteration of the pre-kinematic to synkinematic amphiboles to actinolite (Fig. 12). In Sample 118-733C-1D-1, 10–12 cm, Piece 2, actinolite and chlorite not only fill late crosscutting fractures, but also grow in narrow mylonitic bands, parallel to or slightly oblique to the foliation (Fig. 11). Thus, the deformation of this sample occurred at decreasing temperatures ranging from those of hornblende and cummingtonite stability to those of actinolite and chlorite stability. The geometry of the actinolite plus chlorite mylonitic bands is remarkable: the bands follow an "S"-shaped pattern and have segments both parallel and oblique to the foliation (Fig. 11). The oblique segments are interpreted as shearing segments, with a dextral sense of offset in the thin section (Fig. 11). The same dextral sense of shear is indicated for the earlier, higher-temperature episode by the orientation of extension fractures in the amphibole (Fig. 10).

Sample 118-733D-3B-1, 0-5 cm, Piece 1, is a small pebble of foliated metagabbro that has been intruded by a plagioclase microphenocryst-bearing basalt. The texture of the metagabbro is identical to the other green metagabbros. The crosscutting basalt (dikelet?) is not deformed, and thus its intrusion must postdate the deformation of the metagabbro. The aphanitic matrix of the basalt has been replaced by fine-grained actinolite, similar to the late actinolite replacement observed in the metagabbro. The microphenocrysts are clear, euhedral, and retain igneous twinning.

The fine-grained foliated amphibolite (Sample 118-733D-2D-1, 6–7 cm, Piece 2) contains no relicts of primary igneous minerals. The foliation is marked by crystals of brownish-green hornblende, less than 0.13 mm in size, and by aligned epidote grains, less than 0.01 mm in size. The plagioclase is entirely recrystallized to a mosaic of polygonal grains 0.015 to 0.05 mm in size. All three phases appear to be synkinematic and mutually stable, which suggests an epidote-amphibolite grade of metamorphism. There are no low-temperature alteration minerals.

Characteristic metamorphic assemblages and deformation fabric in the brown metagabbros are discussed next. The brown

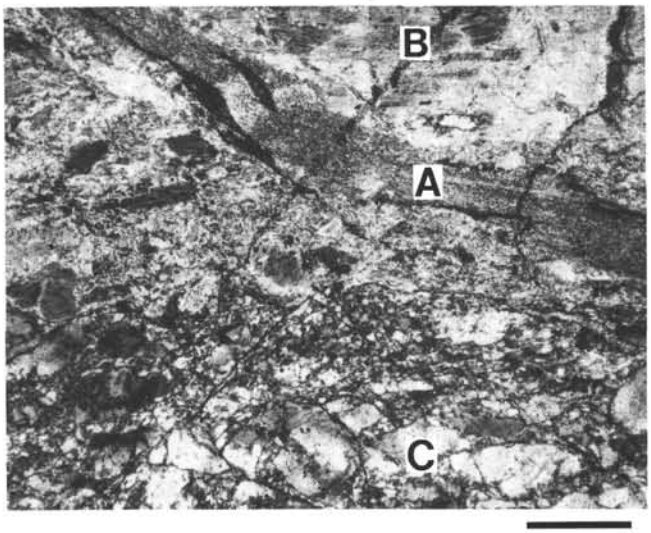

Figure 11. Green metagabbro, Sample 118-733C-1D-1, 10–20 cm, Piece 2. Mylonitic band (A), slightly oblique to the foliation (horizontal in the photograph), and filled with extremely fine-grained actinolite and chlorite. The band is crosscut by a late fracture filled with chlorite (B). Note the crushed and recrystallized plagioclase porphyroclast (C). Crossed nicols, plane light. Scale bar is 0.5 mm.

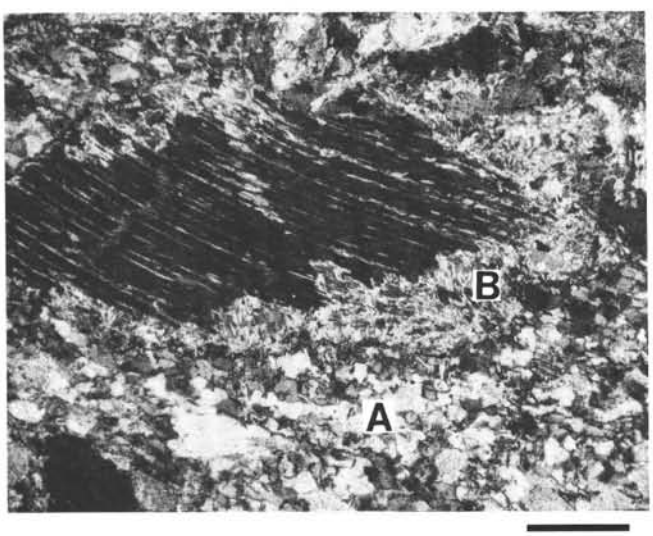

Figure 12. Green metagabbro, Sample 118-733B-1D-1, 0–8 cm, Piece 1. Hornblende crystal elongated in the foliation (horizontal). Note the recrystallized plagioclase (A) and the static alteration of the hornblende rims to actinolite (B). Crossed nicols, plane light. Scale bar is 0.5 mm.

metagabbros (Samples 118-733D-1D-1, 0–46 cm, Pieces 1, 2A, 2B, 3A, and 3B; 118-733D-2D-1, 0–4 cm, Piece 1) all contain porphyroclasts of plagioclase, orthopyroxene, and clinopyroxene, which we interpret as relicts of primary igneous minerals (see "Primary Mineralogy" section, this chapter). These porphyroclasts are plastically deformed and partly recrystallized in polygonal grains. The recrystallized grains themselves are often deformed; thus, the recrystallization is a synkinematic process. The recrystallized assemblage, orthopyroxene plus clinopyroxene plus plagioclase ± brown hornblende, points to high deformation temperatures under anhydrous to slightly hydrous conditions.

A pervasive gneissic foliation and lineation is defined by the elongation of the relict porphyroclasts and of clusters of recrystallized grains. In the two available oriented pieces (Samples 118-733D-1D-1, 14–24 cm, Piece 2B, and 118-733D-1D-1, 32–44 cm, Piece 3B), the foliation dips 45° to 60°, and the lineation appears to dip steeply in the foliation plane.

Igneous plagioclase is as much as 70% recrystallized (mean size of neoblasts: 0.15 mm) and displays tight deformation twins (Fig. 13). Relicts of primary plagioclase are ribbon-shaped porphyroclasts (Fig. 14) and elongated in the foliation. The constant orientation of the mechanical twins relative to the foliation in these ribbon-shaped grains (mechanical twins and foliation make a 50° to 80° angle: see Fig. 14) indicates a strong preferred crystallographic orientation.

The igneous clinopyroxene is 10% to 50% recrystallized (mean size of neoblasts: 0.15 mm), often kinked, and mechanically twinned (Fig. 15). The clear, recrystallized grains cluster around the porphyroclasts and form trails parallel to the foliation. Clear polygonal domains within the clinopyroxene porphyroclasts similarly may be secondary in origin.

The recrystallization of igneous orthopyroxene is limited (about 1%–2% at the most); intracrystalline deformation was the dominant mechanism during the plastic deformation of this mineral. As a result, the orthopyroxene is extremely stretched in the foliation plane (Fig. 16) and shows well-developed preferred crystallographic orientation. In most grains, the (100) intracrystalline slip plane, marked by exsolution lamellae (probably of clinoenstatite), lies near the foliation plane (Fig. 16). The recrystallized orthopyroxene grains (less than 0.1 mm in size) cluster around the porphyroclasts (Fig. 16), or in narrow shear zones parallel to the foliation and cutting through the stretched orthopyroxene porphyroclasts.

Anhedral relicts and blebs of brown hornblende, interpreted as probably igneous (see "Primary Mineralogy" section, this chapter), are locally preserved in the clinopyroxene porphyroclasts. Brown hornblende also can be found as rims around the clinopyroxene porphyroclasts or as interstitial blebs in the clusters of recrystallized clinopyroxenes. These interstitial blebs are themselves sometimes recrystallized into small polygonal grains. These recrystallized grains are metamorphic rather than igneous; they are contemporaneous with the growth of the pyroxene neoblasts during high-temperature plastic deformation.

The relict cores of the clinopyroxene porphyroclasts contain primary igneous cleavage and are filled with inclusions of brown hornblende and opaque grains. Some of the opaque grains (probably ilmenite or titanomagnetite) are replaced by rods and needles of red rutile. The replacement of the titanium oxide phase by rutile instead of sphene is consistent with high-grade metamorphism (Laird, 1982).

Subsequent to the high-temperature plastic deformation, the pyroxenes and brown amphiboles of the brown metagabbros were locally replaced by green amphiboles. Clinopyroxene was replaced by green hornblende and orthopyroxene by a pale amphibole identified optically as cummingtonite (Fig. 17). The replacement appears static; for example, a large crystal of cummingtonite having bent cleavages is in fact a pseudomorph of a deformed orthopyroxene. The green hornblende and cummingtonite crystals are themselves locally replaced by actinolite or actinolitic hornblende. The replacement of pyroxene by amphibole is usually confined to the crystal rims or to crosscutting fractures. The extent of this replacement is greatest near crosscutting veins filled with euhedral green hornblende (Fig. 18). The late shears or fractures within the orthopyroxene are lined with cummingtonite and magnetite. The centers of the larger fractures are filled with green, fibrous actinolite (Fig. 17). The margins of the orthopyroxenes similarly have inner coronas of

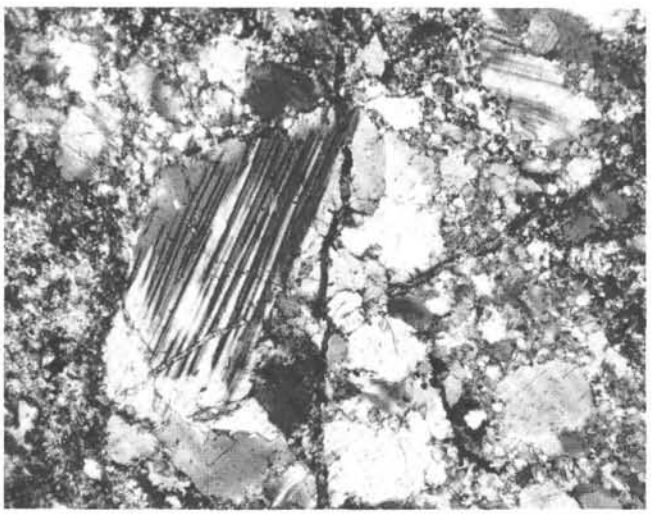

Figure 13. Brown metagabbro, Sample 118-733D-1D-1, 0–7 cm, Piece 1. Partly recrystallized plagioclase porphyroclast having mechanical twins. Crossed nicols, plane light. Scale bar is 0.5 mm.

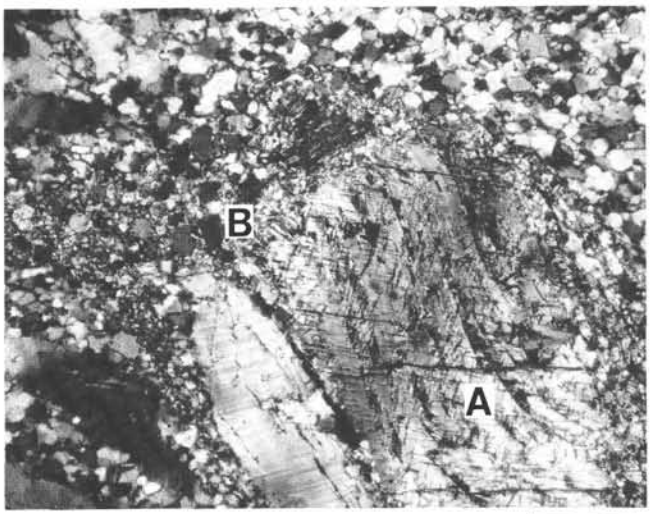

Figure 15. Brown metagabbro, Sample 118-733D-1D-1, 8–13 cm, Piece 2A. Kinked clinopyroxene porphyroclast (A) having a tail of recrystallized clinopyroxene (B). Note the recrystallized plagioclase matrix. Crossed nicols, plane light. Scale bar is 0.5 mm.

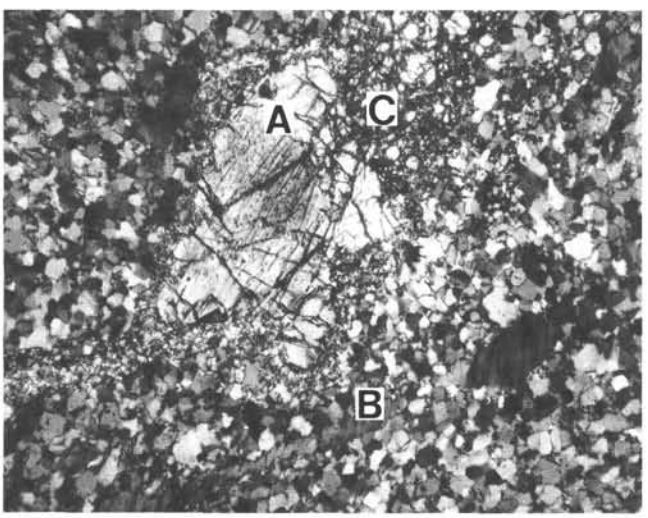

Figure 14. Brown metagabbro, Sample 118-733D-1D-1, 14–25 cm, Piece 2B. Orthopyroxene porphyroclast (A) having tails of recrystallized orthopyroxene (C), in a matrix of recrystallized plagioclase. Note the ribbon-shaped relict (B) of a plagioclase porphyroclast and its mechanical twins. Crossed nicols, plane light. Scale bar is 0.5 mm.

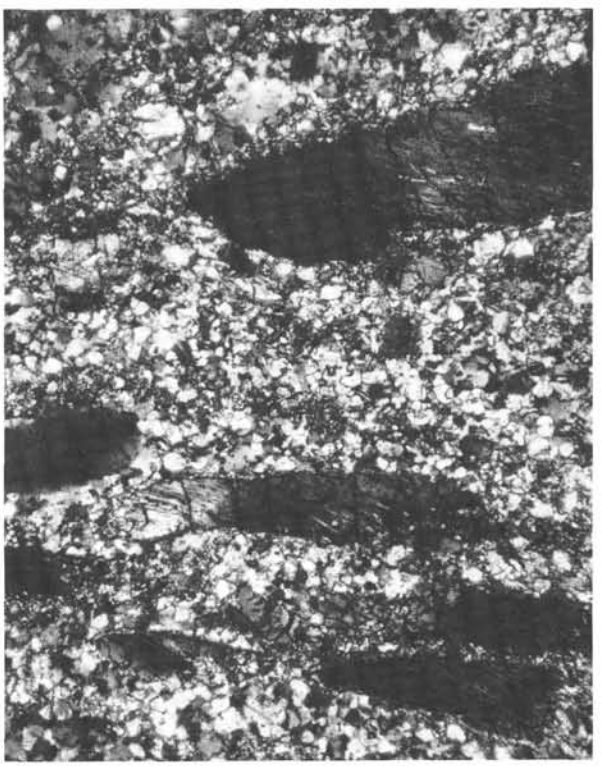

Figure 16. Brown metagabbro, Sample 118-733D-1D-1, 14–25 cm, Piece 2B. Orthopyroxene porphyroclasts stretched in the foliation (horizontal). The (100) slip plane of the orthopyroxene grains, marked by exsolution lamellae (probably of clinoenstatite), are slightly oblique to the foliation: this indicates a dextral sense of shear. Crossed nicols, plane light; Scale bar is 0.5 mm.

cummingtonite and outer coronas of actinolite. Trace amounts of chlorite lie along the boundary between amphibole and plagioclase segregations. These minerals could have formed during brittle fracturing at temperatures lower than those of cummingtonite stability. Alternatively, this assemblage could represent a cogenetic metasomatic front along the grain boundaries. In any case, this nonpervasive, static, middle-grade metamorphism appears linked to the introduction of a fluid phase into the metagabbros. Fluids were introduced to grain boundaries through fractures and veins that crosscut the plastic deformation fabric.

In the metabasalt Sample 118-733C-1D-1, 0–3 cm, Piece 1, the only surviving mafic mineral is represented by a few rounded phenocrysts of olivine (Fig. 19). The groundmass pyroxene crystal and the other mafic phenocrysts (augite and perhaps olivine) are replaced by green actinolite (Fig. 19). Some of the groundmass plagioclase similarly has been replaced by actinolite or actinolitic hornblende. The minimum grade of this pervasive metamorphism is upper greenschist and probably lower amphibolite, as no evidence of replacement of the calcic plagioclase pheno-

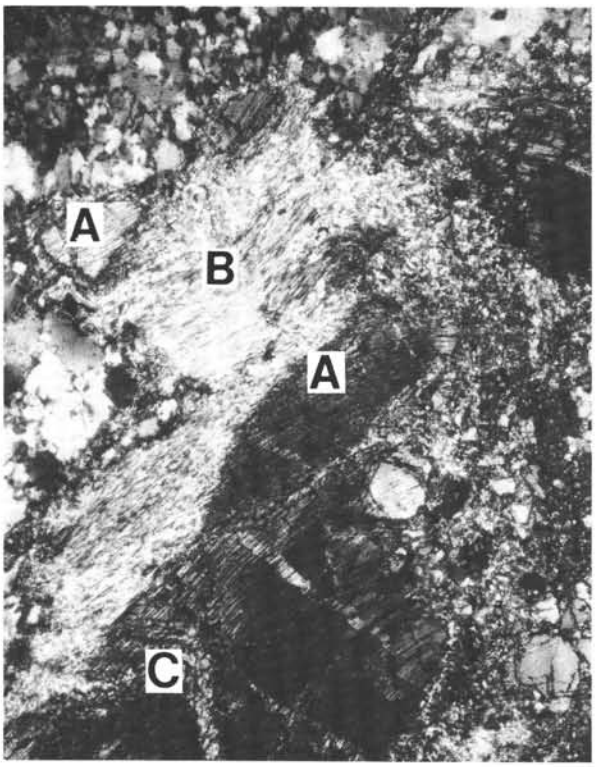

Figure 17. Brown metagabbro, Sample 118-733D-1D-1, 8–13 cm, Piece 2A. Replacement of orthopyroxene (A) by cummingtonite (B). Small fractures (C) in the orthopyroxene are filled with green amphibole (cummingtonite and/or actinolitic hornblende) and opaques. Crossed nicols, plane light. Scale bar is 0.5 mm.

crysts exists (Fig. 19). This metamorphism is similar to that of the glassy basalt intruded into Sample 118-733D-3B-1, 0–5 cm, Piece 1. For this latter sample, the aphanitic mesostasis of the basalt has been replaced by fine-grained actinolite (obvious only adjacent to plagioclase), while the euhedral plagioclase microphenocrysts appear quite fresh.

Conclusions

On petrographic grounds we believe that the gabbronorites and the gabbros are genetically linked. They were probably produced by crystal accumulation from the fractionation of a tholeiitic liquid. This accumulation presumably occurred in a crustal magma chamber at the spreading ridge axis. The composition of the gabbros suggests closed system fractionation; the rocks are intermediate between magnesian cumulates and ferrogabbros. The cumulate nature of the gabbroic rocks requires a depth of origin of approximately 3–5 km (approximately 1 kb of lithostatic pressure). The paucity of hydrous phases in the high-grade assemblages indicates nearly anhydrous conditions for this plastic deformation event. The differential stress during the plastic deformation was presumably of the order of 1–2 kb, from which maximum pressures of 1–3 kb were probably required for the metamorphism.

Metamorphism of Site 733 gabbros and basalts was predominantly retrograde and was associated with deformation and variable seawater penetration. Initial temperatures of metamorphism may have been higher than 700°C (orthopyroxene plus clinopyroxene plus plagioclase ± hornblende assemblage), but this estimate requires accurate phase chemical data. The formation of abundant secondary amphibole suggests a temperature range of 400°–600°C.

Figure 18. Brown metagabbro, Sample 118-733D-1D-1, 14–25 cm, Piece 2B. Late cross-cutting vein filled with green hornblende (A) in porphyroclastic and recrystallized plagioclase. Crossed nicols, plane light. Scale bar is 0.5 mm.

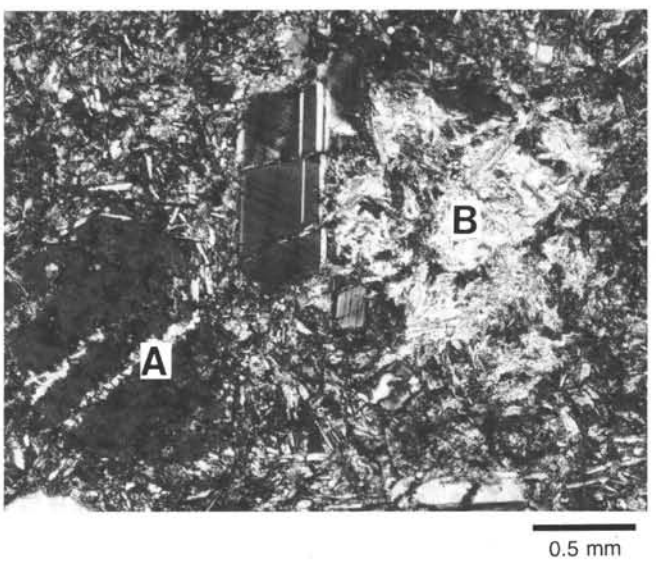

Figure 19. Metabasalt, Sample 118-733C-1D-1, 0–7 cm, Piece 1. Fresh olivine phenocryst (A); mafic phenocryst, altered to green actinolite (B). Groundmass of actinolitized clinopyroxene and plagioclase. Crossed nicols, plane light. Scale bar is 0.5 m.

GEOCHEMISTRY

Two gabbroic rocks from Hole 733D were analyzed by X-ray fluorescence analysis for major oxide compositions and for abundances of some trace elements. The sample preparation technique and analytical procedures are described in the "Introduction and Explanatory Notes" (this volume).

These samples represent two of the gabbro groups established on the basis of thin-section studies (see "Primary Mineralogy" section, this chapter). Sample 118-733D-1D-1, 12–14 cm, Piece 2A, is a gabbronorite and Sample 118-733D-1D-1, 35–37 cm,

Table 3. Chemical compositions of gabbroic rocks from Hole 733D.

Hole:	733D	733D
Section:	1D-1	1D-1
Interval (cm):	12-14	35-37
(in wt%)		
SiO_2	52.99	53.81
TiO_2	0.46	0.53
Al_2O_3	17.67	20.07
Fe_2O_3	6.62	5.24
MnO	0.14	0.11
MgO	6.97	4.53
CaO	12.51	12.14
Na_2O	2.60	3.44
K_2O	0.06	0.06
P_2O_5	0.01	0.02
LOI	+0.19	+0.33
(in ppm)		
V	181	174
Cr	112	32
Ni	48	30
Cu	36	23
Zn	44	35
Rb	0.7	0.4
Sr	134	172
Y	13	13
Zr	17.5	19.2
Nb	1.6	1.4

LOI = Weight loss on ignition.
Note: A weight gain was recorded for both samples.

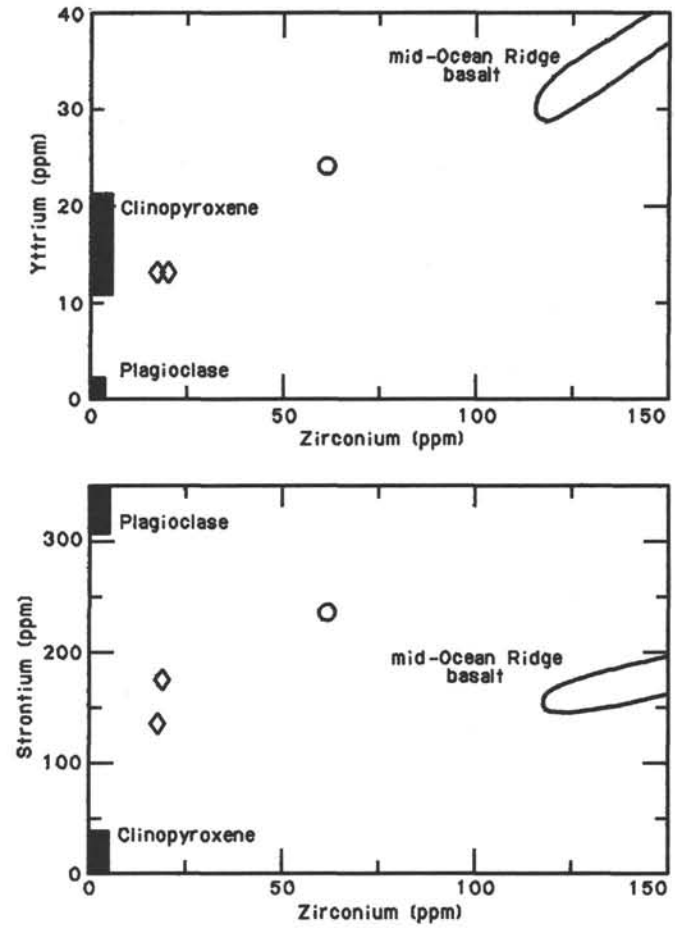

Figure 20. Concentrations of yttrium, strontium, and zirconium in the two analyzed gabbros from Hole 733D (open diamonds). The data for normal Mid-Ocean Ridge basalts and a gabbro (open circle) from Site 732 and estimated concentrations in clinopyroxene and plagioclase in equilibrium with normal Mid-Ocean Ridge basalt liquids are plotted for comparison. The low zirconium contents of the Hole 733D gabbros indicate relatively low amounts of trapped intercumulus liquid, in contrast to the gabbro from Site 732.

Piece 3B, is an orthopyroxene-poor gabbro. The actual modal compositions (in volume percent) of these rocks, as determined by point counting, are given in Table 2. Chemical data are listed in Table 3.

Both samples apparently contain only very small abundances of hydroxyl-bearing minerals (amphiboles, clays, etc.) because they gained weight during ignition. The low contents of MgO, as well as chromium and nickel, and the relatively high SiO_2 concentrations indicate that both rocks crystallized from evolved liquids.

The trace element abundances were mainly determined by the proportions of the two major cumulus phases, clinopyroxene and plagioclase. Concentrations of highly incompatible elements, such as rubidium and zirconium, are up to eight times lower in the gabbros, compared to the basalts of Site 732. Yttrium, strontium, vanadium, and niobium are less depleted in the gabbros, a result of partitioning in clinopyroxene (yttrium), plagioclase (strontium), and oxide phases (vanadium and niobium; Fig. 20). Although the zirconium/niobium, yttrium/zirconium, and yttrium/niobium ratios of the gabbros were slightly affected by crystal accumulation, the values, especially the high yttrium/zirconium and yttrium/niobium ratios, strongly suggest that the gabbros from Hole 733D crystallized from depleted normal-type mid-ocean ridge basaltic melts similar to the clasts recovered at Site 732 (see "Geochemistry" section, Site 732 chapter).

Following a procedure outlined by Meyer et al. (in press), the major oxide data were used to calculate the proportions and compositions of cumulus phases as well as the proportions of trapped liquid for both rock types. The procedure assumes that the rock is composed of an equilibrium assemblage of cumulus minerals plus trapped liquid, and that the liquid has a composition that lies along a liquid line of descent. For the rocks investigated, this liquid line is defined by basaltic compositions from the Southwest Indian Ridge (le Roex et al., 1983), with the limitation that only normal-type mid-ocean ridge basalts having zirconium/niobium ratios greater than 17 were used.

Table 4 shows the calculated bulk compositions; the agreement with actual compositions (Table 3) is very good, except for the substantial differences between the observed and calculated Na_2O contents. The calculated cumulus phase assemblage (in weight percent) for Sample 118-733D-1D-1, 12–14 cm, Piece 2A, is 53.3% plagioclase (An 55.3%), 26.1% clinopyroxene (magnesium value of 73.0), and 12.3% orthopyroxene (magnesium value of 68.9), which is in equilibrium with a liquid having a magnesium value of 38.3. The corresponding values calculated for Sample 118-733D-1D-1, 35–37 cm, Piece 3B, are 62.0% plagioclase (An 51.4%), 20.7% clinopyroxene (magnesium value of 71.5), 5.3% orthopyroxene (magnesium value of 67.3), and a magnesium value of 36.6 for the trapped liquid. The calculated proportions of trapped liquid are 8.4% and 12.4%, respectively, in agreement with estimates based on the contents of a strongly incompatible trace element such as zirconium (Fig. 21). Thus, these rocks are mesocumulates. The data inferred from the calculations are typical of mineral assemblages crystallized from evolved mid-ocean ridge basaltic melts and, once again, underscore the evolved nature of the samples investigated. The calculated mineral proportions are consistent with the modal abun-

Table 4. Calculated compositions of gabbroic rocks from Hole 733D (following Meyer et al., in press; see Table 3 for actual chemical analysis).

Hole:	733D	733D
Section:	1R-1	1R-1
Interval (cm):	12-14	35-37
(in wt%)		
SiO_2	52.89	53.70
TiO_2	0.46	0.51
Al_2O_3	17.74	20.15
FeO_{tot}	6.02	4.79
MgO	7.14	4.70
CaO	12.60	12.22
Na_2O	3.11	3.96
K_2O	0.08	0.11
P_2O_5	0.03	0.04

dances determined by point counting (Table 2), if one allows for the fact that a thin section is not necessarily representative of the larger samples taken for major element analysis.

PALEOMAGNETICS

Introduction

A shipboard paleomagnetic study was conducted to characterize the magnetic properties and to examine the direction of remanent magnetization in highly deformed and altered crustal rocks from Site 733. Although only two vertically oriented samples were recovered at Site 733, it is nevertheless of interest to compare their magnetic properties with those of other oceanic gabbros.

Experimental Methods

Minicores of 2.5 cm in diameter and about 1.4 cm long were drilled from the two oriented pieces of core recovered from Hole 733D. Sample 118-733D-1D-1, 12–14 cm, Piece 2A, is a medium-grained gabbro and Sample 118-733D-1D-1, 35–37 cm, Piece 3B, is a coarse-grained, flaser gabbro. Remanent magnetic properties (intensity, inclination, and declination) were measured with a spinner magnetometer (see "Introduction and Explanatory Notes," this volume). ODP hard-rock cores are not oriented azimuthally, and thus declination values are not meaningful when considered independently.

Alternating field demagnetization (AFD) was performed with a single axis demagnetizer (see "Introduction and Explanatory Notes," this volume), and thus required a separate AFD cycle for each orthogonal axis. Both samples were demagnetized until less than 10% of the original remanence remained (Table 5).

On the basis of demagnetization data, Zijderveld plots were used to identify the stable magnetic inclinations (I_s). The median destructive field (MDF) was determined from the demagnetization curves and represents the peak field at which 50% of the natural remanent magnetization (J_0) was removed. Initial susceptibility (X_0) was measured with a commercial susceptibility meter ("Introduction and Explanatory Notes," this volume). The Koenigsberger (Q) ratio was calculated from observed values of J_0 and X_0 using a 1985 value of the Earth's field at this location (0.38 Oe, Merrill and McElhinny, 1983), so that $Q = J_0/(X_0 \times 0.38)$.

Results

Intensity of Remanent Magnetization (J_0)

J_0 values for Samples 118-733D-1D-1, 12–14 cm, Piece 2A, and 118-733D-1D-1, 35–37 cm, Piece 3B, are 0.75 and 0.45 $\times$ 10^{-3} emu/cm^3, respectively. These values are of the same order of magnitude as those obtained from both unaltered and highly altered oceanic gabbros from the Mid-Atlantic Ridge (Fox and Opdyke, 1973) and unaltered gabbros from the Troodos Ophiolite (Pariso and Johnson, in press).

Initial Susceptibility (X_0)

Susceptibility values for Samples 118-733D-1D-1, 12–14 cm, Piece 2A, and 118-733D-1D-1, 35–37 cm, Piece 3B, are 0.29 and 0.66 $\times$ 10^{-3} cgs units, respectively, and are similar to those obtained by both Fox and Opdyke (1973) and Pariso and Johnson (in press). Both J_0 and X_0 are a function of grain size and concentration of the magnetic minerals within the rock, and it is likely that the low susceptibility values are a result of the small effective magnetic grain size.

Koenigsberger Ratio (Q)

Q ratios for the gabbro and flaser gabbro are 68 and 18, respectively. The Q ratio is a measure of the importance of the remanent magnetization with respect to the *in-situ* induced magnetization, and, in this case, there appears to be negligible induced magnetization. However, we are not sure that the recovered samples are representative of the dominant lithologies in this crustal section. Thus, we could make no generalizations about the source of the *in-situ* magnetization for this crustal section.

Alternating Field Demagnetization (AFD)

The Zijderfeld plots (Figs. 21 and 22) indicate that Sample 118-733D-1D-1, 12–14 cm, Piece 2A, had one component of remanent magnetization and that Sample 118-733D-1D-1, 35–37 cm, Piece 3B, had two components of magnetization. MDF values were determined from the demagnetization curves and were used to judge the stability of magnetization. The MDF value for Sample 118-733D-1D-1, 12–14 cm, Piece 2A, is 300 Oe, which indicates a very stable magnetization. The demagnetization curve for Sample 118-733D-1D-1, 35–37 cm, Piece 3B, shows that a soft, secondary component was removed at a peak field of 150 Oe and that the remaining component is also quite stable (MDF = 280 Oe). The secondary component of this sample may have been acquired during drilling because it was heated during removal from the core barrel.

Inclination

The natural remanent inclinations (I_0) for Samples 118-733D-1D-1, 12–14 cm, Piece 2A, and 118-733D-1D-1, 35–37 cm, Piece 3B, are $-21°$ and $-46°$, respectively. The stable magnetic inclinations (I_s) determined for both samples are approximately $-20°$. Based upon the assumption of a geocentric axial dipole field, the theoretical inclination value for 33°S latitude is $-52°$. The anomalous inclination values may be explained by one or more of the following mechanisms: (1) tectonic rotation of a crustal block, (2) gravitational displacement and rotation of a large boulder, (3) paleosecular variation, or (4) post-cooling southern drift of the crust from which the sample was taken. Once again, we found it difficult to reach a conclusion based on only two samples, and further studies will be necessary to understand the remanent magnetic properties of the rocks recovered from this site.

PHYSICAL PROPERTIES

Two cylindrical minicores were cut perpendicular to the splitting plane for shipboard analysis of grain density, porosity, and velocity (Table 6). The small percentage of porosity is associated with microfractures distributed throughout the rock. Grain densities are completely consistent with the mineral proportions and densities. In contrast, the observed compressional wave velocities are lower than expected from the isotropic mineral ve-

Table 5. Remanent magnetic properties for stepwise demagnetization.

Core/section interval (cm)	Depth (mbsf)	AF (Oe)	CSD (degrees)	Dec. (degrees)	Inc. (degrees)	Intensity (mA/m)
118-733D-1D-1, 12	15.12	000	4.6	350.0	−21.2	750.4120
1D-1, 12	15.12	025A	4.6	349.1	−21.2	728.1910
1D-1, 12	15.12	050A	5.9	348.5	−19.3	695.4000
1D-1, 12	15.12	075A	6.3	347.7	−20.0	660.9790
1D-1, 12	15.12	100A	7.0	347.0	−20.4	619.2450
1D-1, 12	15.12	150A	6.2	346.5	−17.3	527.9690
1D-1, 12	15.12	200A	7.7	345.8	−18.4	461.9980
1D-1, 12	15.12	250A	8.1	345.2	−18.7	402.4070
1D-1, 12	15.12	300A	8.4	345.3	−19.1	352.9150
1D-1, 12	15.12	350A	8.5	345.3	−18.1	309.9240
1D-1, 12	15.12	400A	7.7	346.8	−18.6	270.9870
1D-1, 12	15.12	500A	8.4	348.0	−18.8	212.1780
1D-1, 12	15.12	600A	8.3	348.0	−19.1	168.2290
1D-1, 12	15.12	700A	8.7	350.7	−21.9	134.5870
1D-1, 12	15.12	800A	8.7	355.0	−24.8	108.7010
1D-1, 12	15.12	900A	6.8	11.1	−38.5	94.0149
1D-1, 35	15.35	000	9.3	21.3	−46.4	445.7980
1D-1, 35	15.35	025A	6.1	11.3	−39.3	422.0560
1D-1, 35	15.35	050A	4.7	7.6	−32.5	385.7800
1D-1, 35	15.35	075A	4.0	7.4	−28.2	355.0460
1D-1, 35	15.35	100A	4.3	6.9	−25.4	331.8210
1D-1, 35	15.35	150A	4.9	6.2	−22.5	291.9200
1D-1, 35	15.35	200A	4.2	6.3	−21.4	257.6520
1D-1, 35	15.35	250A	3.8	6.7	−20.1	226.9090
1D-1, 35	15.35	300A	4.5	6.7	−20.2	204.0300
1D-1, 35	15.35	350A	4.9	6.1	−19.4	182.6250
1D-1, 35	15.35	400A	5.4	5.2	−19.8	163.6080
1D-1, 35	15.35	500A	5.0	6.5	−18.7	130.6780
1D-1, 35	15.35	600A	5.5	6.9	−18.4	103.8300
1D-1, 35	15.35	700A	5.4	10.0	−19.9	77.7334
1D-1, 35	15.35	800A	7.0	7.8	−20.8	60.2040

Mbsf = depth below seafloor, including the 15 m of overlying sediment; AF = peak demagnetizing field; CSD = circular standard deviation; Dec. = declination; Inc. = inclination; and Intensity = magnetic intensity.

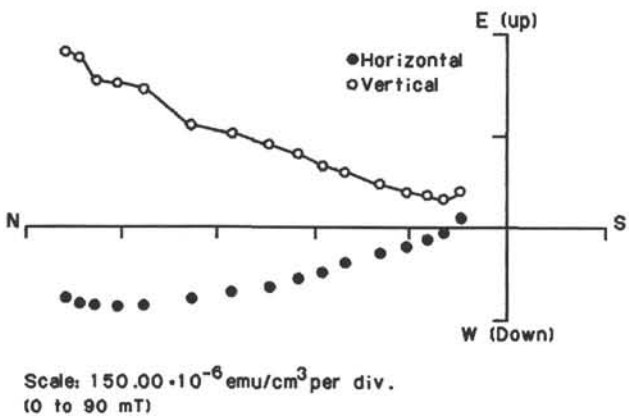

Figure 21. Zijderfeld plot showing the horizontal and vertical magnetic vectors during stepwise demagnetization.

locities and densities (Fig. 23). Three explanations of this discrepancy may apply.

1. The direction in which velocities were measured is not representative of the average V_p of the two rocks measured because of a possible V_p anisotropy.
2. The fracture porosity of the two metagabbros may have reduced the compressional wave velocity. Gabbroic rocks, as well as most other igneous rocks, tend to show an increase in V_p of about 0.2–0.5 km/s (Christensen, 1982), with an increase in pressure that is attributed to the closure of microcracks.
3. The single-crystal velocities used for comparison with the rock velocities are inappropriate for the mineral compositions in the rocks under study. This seems to be unlikely considering the mineral compositions in these rocks.

The principal secondary mineral in these rocks is hornblende (see "Primary Mineralogy" section, this chapter), with only trace amounts (1%–2%) of phyllosilicates. Metagabbros from other fracture zones, such as the Kane and the Oceanographer fracture zones, commonly have velocities that are substantially lower than those determined here, even when they have relatively similar densities (Fig. 24). Alteration to lower metamorphic grade might reduce V_p by replacing the primary minerals with phyllosilicates that have lower V_p (Fig. 23).

Thermal conductivity was measured on one metagabbro sample from Site 733 (Sample 118-733-1D-1, 38–45 cm, Piece 3B). A slab with approximate dimensions (10 × 50 × 70 mm) was cut perpendicular to the plane of gneissic foliation, which inclined approximately 45° to the axis of a continuous 130-mm-long section of core. This slab was ground flat to a 600 grit finish, and thermal conductivity was measured using the needle probe method adapted to a slab sample configuration, as described by Von Herzen and Maxwell (1959) and Vacquier (1985). This technique measures the thermal conductivity (K) radial to the probe, excluding the heat transfer parallel to the probe, so that variations in thermal conductivity with probe orientation are rough indicators of anisotropies in conductivity caused by preferred mineral orientations. We observed variations in K within the plane of the slab cut parallel to the core axis and perpendicular to foliation (Table 7). Reproducibility of conductivity standards with similar K values was within about 0.05 W/m/K and thus the directional variations in K are probably real and stem from preferred mineral orientation. Lack of specific information on the thermal conductivity tensors for plagioclase, orthopyroxenes, and clinopyroxenes and the preferred mineral orientations in the sample preclude a more quantitative interpreta-

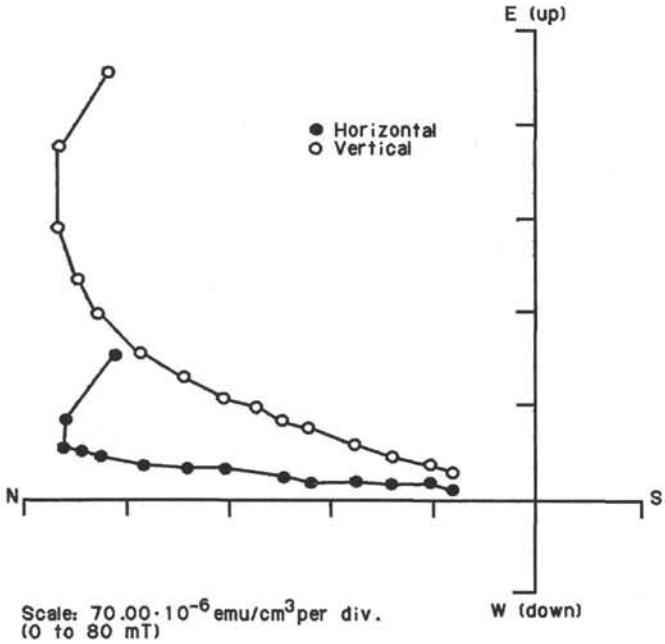

Figure 22. Zijderfeld plot showing the horizontal and vertical magnetic vectors during step-wise demagnetization. Two magnetic components are present, and the curvature between them indicates an overlapping of the coercivity spectra.

Table 6. Summary of the physical properties of samples recovered from Site 733.

Core/section interval (cm)	Texture and lithology	Grain density (Mg/m^3)	Porosity (%)	Velocity (km/s)
118-733D-1D-1, 12–14	Gneissic metagabbro	2.960 [a](2.920)	0.5	6.24 [a](6.84)
1D-1, 35–37	Gneissic metagabbro	2.870 [a](2.810)	0.4	6.14 [a](6.66)

[a] Densities and compressional-wave velocities, in parentheses, calculated from the percentages of minerals (Table 2) and single-crystal properties shown in Figure 24.

tion of these variations in K with direction. The mean conductivity of 2.05 ± 0.1 W/m/K is typical of rocks of similar gross mineralogy, such as diabases and gabbros that have K values ranging from 1.7 to 2.5 W/m/K (Clark, 1966). These conductivities are low when compared to granites, granodiorites, and ultramafic rocks and reflect the low conductivity of plagioclase feldspar (1.8 ± 0.1 W/m/K, Clark, 1966), which is the predominant mineral in this sample.

SUMMARY AND CONCLUSIONS

Site 733 is located on the west wall of the Atlantis II transform at about 33°05′S, 56°59′E, in an area where peridotite was dredged during the site survey. Several flat benches in the area offered potential sites for deployment of the hard-rock guidebase, should peridotite be located during test spud-ins. During a television/sonar survey, two areas were identified as potentially suitable drilling sites: a flat, sedimented bench in 4483 m of water and a small sediment-filled trough about 700 m farther downslope in 5208 m of water. No good bare-rock outcrops were located during the survey, but basement was thought to underlie the sedimented areas at shallow levels.

Four holes were drilled in these two locations, the deepest of which penetrated 23.5 mbsf. Holes 733A, 733B, and 733C are

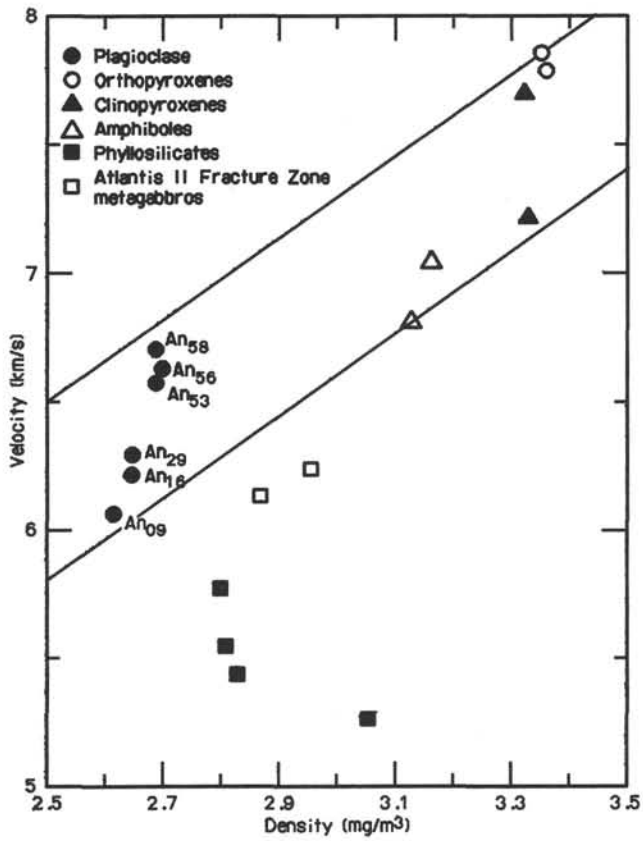

Figure 23. Velocity vs. density systematics for mafic minerals and the data for the two Atlantis II Fracture Zone metagabbro samples. Arrows indicate the likely range of velocity and density correction for fracture porosity. Note the substantially lower velocities for phyllosilicates that would lower bulk velocities for low-grade alteration gabbros. Lines represent the approximate bounds on the velocity and density for the metagabbros, based on the properties of the component minerals. Data from Christensen (1982).

located on the upper bench and were test holes drilled a few meters apart. A total of 0.29 m of material was obtained from Holes 733B and 733C for an average recovery of 2.1%. Hole 733D, drilled in the lower trough, was washed to a depth of 15 mbsf and then drilled to 23.5 mbsf. Less than 0.5 m of material was recovered from this hole.

The material recovered from Holes 733B and 733C consists entirely of fragments of foliated metagabbro and amphibolite, none of which were actually cut by the bit. The size and shape of the fragments indicate that they represent talus deposits, not basement. Foliated metagabbro, amphibolite, and minor basalt were recovered in Hole 733D. Although a short whole-round piece of metagabbro was recovered, it probably came from a boulder in the talus pile, rather than from basement.

The foliated metagabbros and amphibolites were subjected to high-temperature plastic deformation and were extensively recrystallized. Two types of metagabbro are present: a green variety composed chiefly of amphibole and plagioclase and a brown variety that contains mostly pyroxene and plagioclase. We believe that the protoliths for both varieties are an orthopyroxene-rich ferrogabbro. The amphibolite is strongly foliated and consists of amphibole, plagioclase, and epidote. In the metabasalt, actinolite replaces most of the mafic minerals and some of the groundmass plagioclase. Chlorite and epidote are absent, which suggests upper greenschist to lower amphibolite facies conditions of metamorphism.

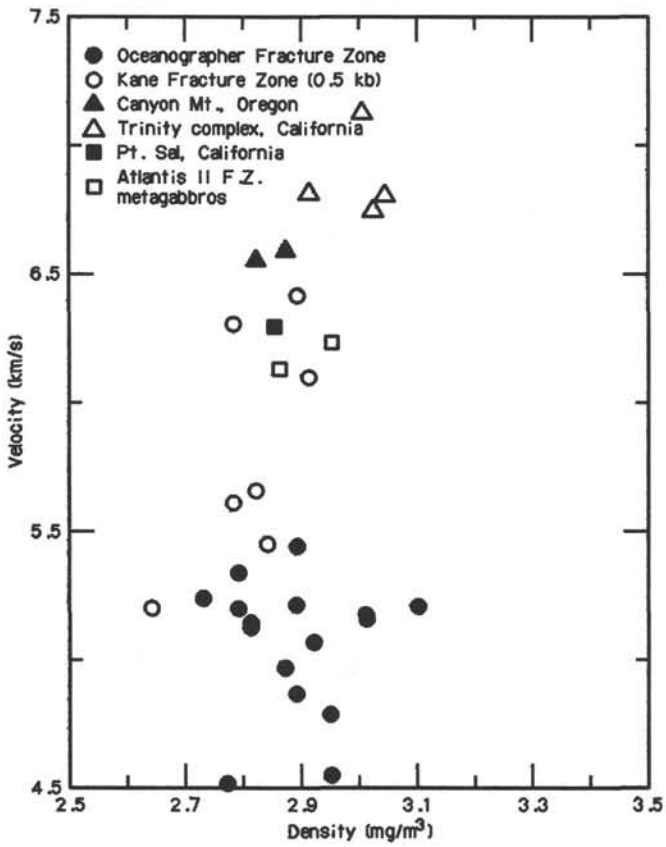

Figure 24. Velocity vs. density data for metagabbros, including the two Atlantis II metagabbro samples under study. Note the significantly lower velocities of metagabbros at various fracture zones, which we interpreted as consequence of lower-grade alteration to assemblages, including phyllosilicates. Data from Christensen (1982).

Table 7. Summary of variations in thermal conductivity with direction in Sample 118-733D-1D-1, 38–45 cm, Piece 3B.

Probe direction	Conductivity (W/m/K)
Parallel to core axis	2.16
Parallel to foliation (45° to core axis)	2.00
Normal to foliation (−45° to core axis)	1.98

The metagabbros from Hole 733D have remanent magnetic intensities similar to those of fresh and altered gabbro from the Mid-Atlantic Ridge but have much lower initial susceptibilities. The stable magnetic inclinations average from −20°, but this has little significance because the core was probably recovered from a boulder in talus overlying basement.

Measured grain densities of the metagabbros are 2.87 and 2.96 g/cm^3, within the range of expected values. However, the compressional-wave velocities (6.14–6.24 km/s) are somewhat higher than those for metagabbros from other fracture zones. The low values may be due to differing types or amounts of alteration or to varying proportions of microcracks.

Thermal conductivities range from 1.98 to 2.16 W/m/K and vary systematically when measured parallel or normal to the foliation. The mean conductivity of 2.10 ± 0.10 W/m/K is typical for diabase and gabbros. We believe that the observed anisotropy reflects preferred mineral orientations.

The television/sonar survey conducted at Site 733 demonstrated that both the steep slopes and benches on the transform wall are covered with talus and rubble. Variable thicknesses of finer-grained sediment have also accumulated on the flat benches. The benches observed at Site 733 are probably fault controlled, but the sedimented trough at the foot of the slope (Hole 733D) may have been formed by slumping or landsliding.

Drilling was very difficult in the loose talus and sediment because of poor hole stability. The unconsolidated sediment seemed to wash away during drilling, and only small, pebble-sized fragments were recovered. Larger boulders, such as the one penetrated in Hole 733D, might have been cored if the sediments were somewhat more coherent.

The complete absence of peridotite in the recovered material suggests that only gabbro and metagabbro are present on this part of the transform wall.

REFERENCES

Cann, J. R., 1979. Metamorphism in the oceanic crust. *In* Talwani, M., Harrison, C. G., and Hayes, D. E. (Eds.), *Deep Drilling Results in the Atlantic Ocean: Ocean Crust*: Washington (Am. Geophys. Union, Maurice Ewing Ser. 2), 230–238.

Christensen, N. I., 1982. Seismic velocities. *In* Carmichael, R. S. (Ed.) *Handbook of Physical Properties of Rocks*, Vol II: Boca Raton, FL (CRC Press), 1–228.

Clark, S. P., Jr., 1966. Thermal conductivity. *In* Clark, S. P., Jr. (Ed.), *Handbook of Physical Constants*: Alexandria, VA (Geol. Soc. Am.), Mem. 97:459–482.

Fox, P. J., and Opdyke, N. D., 1973. Geology of the oceanic crust: magnetic properties of oceanic rocks. *J. Geophys. Res.*, 78:5139–5154.

Laird, J., 1982. Amphiboles in metamorphosed basaltic rocks: greenschist to amphibolite facies. *In* Veblen, D. R., and Ribbe, P. H. (Eds.), *Amphiboles: Petrology and Experimental Phase Relations*: (Mineral. Soc. Am., Rev. in Mineral.), 9B:113–135.

le Roex, A. P., Dick, H.B.J., Erlank, A. J., Reid, A. M., Frey, F. A., and Hart, S. R., 1983. Geochemistry, mineralogy and petrogenesis of lavas erupted along the Southwest Indian Ridge between the Bouvet Triple Junction and 11 degrees east. *J. Petrol.*, 24:267–318.

Merrill, R. T., and McElhinny, M. W., 1983. *The Earth's Magnetic Field*: London (Academic Press).

Meyer, P. S., Dick, H.B.J., and Thompson, J., in press. Cumulate gabbros from the Southwest Indian Ridge 54°S, 7°E. *Contrib. Mineral. Petrol.*

Pariso, J. E., and Johnson, H. P., in press. Magnetic properties of an analog of the lower oceanic crust: magnetic logging and paleomagnetic measurements from drillhole CY-4 in the Troodos Ophiolite. *Init. Repts. Cyprus Crustal Study Proj.*, Hole CY-4.

Streckeisen, A. 1976. To each plutonic rock its proper name. *Earth-Sci. Rev.*, 12:1–33.

Vacquier, V., 1985, The measurement of thermal conductivity of solids with a transient linear heat source on the plane surface of a poorly conducting body. *Earth Planet. Sci. Lett.*, 74:275–279.

Von Herzen, R. P., and Maxwell, A. E., 1959. The measurement of thermal conductivity of deep sea sediments. *J. Geophys. Res.*, 65: 1535–1541.

Ms 118A-105